# Towards low-cost context awareness on smart shelving using passive UHF RFID infrastructure

by

Heyi Li

B.S., Microelectronics, Southern University of Science and Technology (2021)

Submitted to the Department of Mechanical Engineering
in partial fulfillment of the requirements for the degree of

Master of Science in Mechanical Engineering

at the

MASSACHUSETTS INSTITUTE OF TECHNOLOGY

June 2023



Author .....
Department of Mechanical Engineering
May 19, 2023

Certified by .....
Sanjay Sarma
Professor of Mechanical Engineering
Thesis Supervisor

Accepted by .....
Nicolas G. Hadjiconstantinou
Chairman, Department Committee on Graduate Theses

**Towards low-cost context awareness on smart shelving using passive UHF RFID infrastructure**

by

Heyi Li

Submitted to the Department of Mechanical Engineering
on May 19, 2023, in partial fulfillment of the
requirements for the degree of
Master of Science in Mechanical Engineering

## Abstract

An omni-channel strategy is a method of selling and promoting products that offers customers a comprehensive and cohesive shopping experience. However, this strategy relies on store managers having an accurate, real-time understanding of product availability at all their distribution and retail facilities. Smart shelving is an important avenue for furthering the development of omni-channel retailing and meeting people's needs. This thesis primarily focuses on the construction of a low-cost context awareness infrastructure for smart shelving using passive UHF RFID tags and radio tomographic imaging (RTI) algorithms.

Firstly, location estimations without fingerprinting in one direction can reach an accuracy of 91.7% on four tested objects. Secondly, the number of stacked layers from 1-3 when placing items on the shelf can be estimated. It is shown that an increase in product volume on the shelf could be related to tag RSSI level changes for five different tested products.

In addition, material classification could be achieved by tag RSSI attenuations. Tests are done between three classes (metal, glass, and plastic), with three objects each class. In the three-location tests, it is possible to clearly differentiate between three types of materials based on the value of variations in tag RSSI attenuations.

Finally, the integration of battery-free environmental sensors is accomplished by incorporating an RFID tag equipped with resistance measurement capability and a photoresistor. By measuring the resistance of the photoresistor, the designed light sensor could provide additional information (besides the tag RSSI change) about the volume of material on a shelf. Moreover, this can be done using only a single UHF RFID Gen 2 protocol.

Thesis Supervisor: Sanjay Sarma
Title: Professor of Mechanical Engineering

# Acknowledgments

I would like to express my deepest gratitude to my advisor, Sanjay Sarma, for his guidance, expertise, and unwavering support throughout my master's study. Sanjay not only provided guidance in technical matters but also encouraged me to explore the possibilities of future research and discover innovative aspects of everyday life. This greatly broadened my perspective as a master's student and gave me the courage to think and act boldly in my future endeavors. In addition, Sanjay cares deeply for the members of the Auto-ID lab and his humorous demeanor creates a joyful atmosphere among us. I am truly grateful for his mentorship and the opportunity to work under his supervision.

I would like to express my gratitude to the Research Scientist of Auto-ID lab, Rahul Bhattacharyya. Rahul has provided tremendous support throughout my entire thesis. From generating ideas to designing experiments and attending to every detail, he has been willing to offer advice and assistance. During our weekly meetings, we always engage in productive and meaningful discussions that have propelled the progress of my research. His shared knowledge, discussions, and feedback have enriched my research experience and aided in the development of this thesis.

I am also thankful to the members of Auto-ID lab. Everyone is supportive, collaborative, friendly, and warm. Each person has their own unique research focus, which fosters a free and diverse research environment that provides ample opportunities for collaboration among members.

I am grateful to my friends. As an international student, I consider myself fortunate to have found such wonderful friends with whom I have spent enjoyable leisure time. Socializing and engaging in sports are integral parts of my life, and I hope our bond will continue to grow.

I want to express my heartfelt gratitude to my parents and families. Their care, love, and support have been my greatest motivation and a source of strength during challenging times. I wish them a continued life filled with health and happiness.

Lastly, I want to extend my thanks to MIT. I never imagined that my master's

studies would be so enriching and joyful. This is thanks to the abundant resources provided by the university and the teachers and staff who have always been there to assist me.

# Contents

**1 Introduction** **15**

**2 Promising application fields of the proposed system** **17**

2.1 Omni-channel retailing . . . . . 17

2.2 Smart shelves . . . . . 18

2.2.1 Real-time merchandise tracking . . . . . 22

2.2.2 Stocks tracking . . . . . 23

2.2.3 Material classification . . . . . 24

**3 Existing related research work** **27**

3.1 UHF RFID localization . . . . . 27

3.2 UHF RFID sensing . . . . . 28

**4 Basics of RFID technology** **31**

4.1 History of RFID . . . . . 31

4.2 Types of RFID . . . . . 32

4.3 Radio basics of UHF RFID . . . . . 32

4.3.1 UHF RFID and its current applications . . . . . 32

4.3.2 Radio Basics . . . . . 33

**5 Methodologies and experiment design** **43**

5.1 RTI mechanism . . . . . 43

5.2 Weight model . . . . . 48

5.3 Regularization for ill-posed problems . . . . . 49

5.4 Test setup . . . . . 52
5.5 Design problems . . . . . 54
5.6 Measurement signal . . . . . 57
5.7 Parameter optimization . . . . . 58

**6 Results** **61**

6.1 Location estimation without fingerprinting . . . . . 61
6.2 Stocks monitor and auto-stock reminder . . . . . 65
6.3 Material classification by tag RSSI attenuation . . . . . 71
6.4 Battery-free environmental sensors . . . . . 76

**7 Conclusions and future work** **87**

7.1 Conclusion . . . . . 87
7.2 Future work . . . . . 88

# List of Figures


2-1 Omni-channel retailing . . . . . 18
2-2 Placement of Zed 2 camera above the tested area . . . . . 20
2-3 Camera view when pasta boxes are stacked from 1 to 3 . . . . . 21
2-4 Camera view when one metal can (right) and one glass can (left) are put in the area . . . . . 22

4-1 Pulse-interval encoding . . . . . 34
4-2 Backscattered link . . . . . 35
4-3 Reader symbols . . . . . 39

5-1 Illustration of RTI network. Radio links are between wireless nodes and weights could be distributed to each voxel in the tested region. . 45
5-2 pRFID based RTI network where links are between antenna and RFID transponders. . . . . 47
5-3 Illustration of weighting model . . . . . 48
5-4 Test setting environment . . . . . 53
5-5 Placement of antennas and UHF RFID tags . . . . . 54
5-6 Each pixel could be thought as a water reservoir. Every link passing by could add a water valve to it, by which the open position of valve is controlled by weight assigned to that particular pixel. . . . . 55
5-7 Two different placements of antennas . . . . . 56
5-8 RSSI vs. frequency in 902.75 – 927.25 MHz of one antenna reading one tag . . . . . 57
5-9 Two prior positions for parameter optimization . . . . . 59

6-1 Illustration of three pre-defined positions . . . . . 61
6-2 Objects whose location to be estimated . . . . . 62
6-3 Real testing cases for three positions (left: 1, right: 2, bottom: 3 in Figure 6-1) . . . . . 62
6-4 Position estimation of four different objects at three positions . . . . 63
6-5 Attenuation values in each heat map of Figure 6-4 . . . . . 64
6-6 Height refence of tested objects, whose length varies from 8cm to 20cm 66
6-7 Heat map for five different types of objects from 1 to 3 stacks (Animal cracker) . . . . . 67
6-8 Heat map for five different types of objects from 1 to 3 stacks (Milkshake) 67
6-9 Heat map for five different types of objects from 1 to 3 stacks (Pasta) 68
6-10 Heat map for five different types of objects from 1 to 3 stacks (Sugar) 68
6-11 Heat map for five different types of objects from 1 to 3 stacks (Sweetener) 69
6-12 Attenuation for five types of objects from 1 to 3 stacks . . . . . 69
6-13 Relationship between sum of attenuations and total number of objects on shelf . . . . . 70
6-14 Different numbers of objects being placed on shelf . . . . . 70
6-15 Test sets from plastic, glass and metal class . . . . . 71
6-16 Attenuation of three materials (three objects for each material) at position 1 . . . . . 72
6-17 Attenuation of three materials (three objects for each material) at position 2 . . . . . 73
6-18 Attenuation of three materials (three objects for each material) at position 3 . . . . . 74
6-19 By averaging all maximum attenuation values of measurements of one type of material, classifications could be done according to relative relationship between materials. . . . . 75
6-20 SPI protocol . . . . . 77
6-21 Communication within RFID sensor . . . . . 78

6-22 In Impinj software, user could read contents from a tag's memory after specifying EPC of the tag. . . . . 78
6-23 Example of reading 4 words start from address 256 from User bank . 79
6-24 Example of a valid resistance measurement data with ItemTest . . . . 79
6-25 QOS bits could indicate the validity of sensor data. . . . . 80
6-26 Rocky100 connected to a photoresistor . . . . . 81
6-27 Placement of light sensor and direction of light . . . . . 81
6-28 Resistance of photoresistor under different lighting. Small flashlight means taking the flashlight of cellphone away at around 50 cm and shine at the photoresistor. Big flashlight means that it shines from close up at the sensor. . . . . 82
6-29 Situation when two stacks of boxes are placed in front of the photoresistor 83
6-30 Resistance of photoresistor when one to three stacks of boxes are placed in the front . . . . . 83
6-31 Resistance vs. total number of objects. Numbers could also indicate the maximum layer on the shelf. . . . . 84
6-32 Three tested combinations for total number of 6 objects . . . . . 85

# List of Tables

5.1 The parameters to obtain the maximum accuracy of the two tested positions . . . . . 59

6.1 Location estimations for plastic, glass and metal tested in three locations 71

6.2 Averaged maximum attenuation value for plastic, glass and metal tested in three locations . . . . . 75

# Chapter 1

# Introduction

Omnichannel retailing refers to a comprehensive approach that seamlessly integrates multiple channels and touchpoints to provide customers with a unified and personalized shopping experience. Smart shelves play a crucial role in omni-channel retailing by leveraging advanced technology to provide real-time inventory tracking, personalized product recommendations, and seamless integration with online platforms, enhancing the overall customer experience across multiple channels.

The two most common technologies used to implement smart shelves are computer vision (CV) and radio frequency identification (RFID). CV offers effective automated visual recognition and analysis of products, but it still has limitations in accurately interpreting depth, handling challenging lighting conditions and occlusions, and distinguishing objects with similar shapes or appearances, impacting its overall performance and reliability in practical applications. Moreover, the extensive deployment of cameras in data collection substantially escalates the costs related to implementing computer vision technology. Conversely, RFID presents a cost-effective solution for supporting smart shelves, primarily emphasizing object interaction detection rather than offering comprehensive item information encompassing precise positioning, approximate quantity, or material composition.

This thesis serves as an exemplification of a low-cost RFID sensing technology that can be integrated with other shelf sensing technologies, aiming to enhance context awareness, reduce data collection requirements, and minimize overall costs. The

proposed RFID-based smart shelf awareness system focuses on three primary objectives: "real-time merchandise tracking", "stock tracking" and "material classification". These goals are accomplished through the implementation of localization and sensing techniques within a unified RF protocol.

Regarding RFID localization, both range-based and range-free approaches have been investigated. While range-based methods offer relatively precise location detection, they often suffer from high computational complexity. On the other hand, range-free approaches, such as fingerprinting and Radio Tomographic Imaging (RTI), have been developed. However, fingerprinting localization is susceptible to environmental changes, requires extensive calibration, and exhibits limited scalability. Moreover, RTI algorithms have not been widely utilized in small-scale applications, typically confined to outdoor areas of approximately 50 square meters.

Although RFID sensing typically relies on independent RFID-based sensors to provide information, it lacks the capability to simultaneously transmit data from other RFID tags that are not specifically designated as sensors with the same protocol.

In addressing these limitations, this thesis proposes a range-free, non-fingerprinting, UHF RFID-based system with RTI implementation for indoor smart shelf applications and small-scale environments. The obtained results are employed for location estimation, stocks monitoring, material classification, and environmental sensing, all under the Class 1 Gen 2 protocol.

The subsequent sections of this thesis will be organized as follows: Chapter 2 provides an introduction to the background and promising application fields of the proposed system. Chapter 3 presents an overview of the existing research work on RFID localization and sensing. Chapter 4 delves into the fundamental principles of RFID and its relevance to the RF communication of the proposed system. Chapter 5 details the methodologies and experimental design employed in this project. Chapter 6 presents the measurement results obtained, and Chapter 7 encompasses the concluding remarks and outlines future directions for research.

# Chapter 2

# Promising application fields of the proposed system

## 2.1 Omni-channel retailing

As the background of the thesis, omni-channel retailing refers to a business strategy that aims to provide a seamless shopping experience to customers across multiple channels, such as online, mobile, and physical stores (Figure 2-1). This means that customers can shop and interact with the retailer through various channels, and expect a consistent and personalized experience regardless of the channel they use [1, 2, 3, 4]. According to Mckinsey's report in 2021, since the onset of the pandemic, over 33% of the American population has incorporated omnichannel capabilities, such as online purchases followed by in-store pickups, into their regular shopping practices. Furthermore, nearly 66% of these individuals express intentions to sustain this behavior in the future [5].

After customers have successfully identified the desired product for purchase, they commonly proceed to the purchasing stage. At this point, customers have the flexibility to make their purchases through various channels, such as a retailer's website, an online marketplace, or even a brick-and-mortar store.

One of the key drivers behind the development of omni-channel retailing is the rise of mobile technology [6, 7]. With the widespread adoption of smartphones and


Figure 2-1: Omni-channel retailing

tablets, customers now have access to a range of digital devices which are various channels to interact with retailers. This has created new opportunities for retailers to engage with customers and offer personalized shopping experiences. Another driving factor is the increasing importance of customer experience in the retail industry. Customers today expect a high level of convenience, choice, and personalization from retailers. By providing a seamless omni-channel experience, retailers can meet these expectations and build long-term customer loyalty.

Smart shelves, which are equipped with sensors and cameras or other technologies that enable retailers to track inventory levels, analyze customer behavior, and deliver personalized promotions in real-time is one of the key technologies enabling omni-channel retailing.

## 2.2 Smart shelves

As the approach this thesis to add to omni-channel retailing, smart shelves allow retailers to more effectively manage their inventory and improve their supply chain efficiency. By providing real-time data on inventory levels, smart shelves enable retailers to restock their products more quickly and accurately, reducing the likelihood of out-of-stock situations. This is particularly important in the era of omni-channel

retailing, where customers expect to be able to order products online and pick them up in-store or have them delivered quickly to their homes. Smart shelves are also able to increase supply chain efficiency, improve inventory management, and enhance customer engagement and loyalty. As the retail industry continues to evolve and customers become more demanding in their expectations, smart shelves will likely play an increasingly important role in enabling retailers to deliver the seamless, personalized shopping experience that customers expect.

As an example, Amazon Go is a revolutionary retail concept that leverages advanced computer vision and machine learning technologies to create a checkout-free shopping experience. With Amazon Go, customers can walk into a store, pick up items they want to purchase, and leave without having to go through a traditional checkout process.

There are several technologies currently being used in the development of smart shelves. Research works including RFID have been done to track inventory levels and monitor customer behavior. Medeiros et al. [8] present an RFID-based low-cost smart shelf for book identification at UHF. Hrebenciuc et al. [9] proposed an RFID low-cost system for large setups of shelves. Joan Melià-Seguí and Rafael Pous implemented the classification of human interaction on a real smart shelf according to RFID features [10]. Another recent technology that has been used in smart shelves is computer vision. This technology uses cameras and image processing algorithms to recognize and track products in real time. This allows for accurate tracking of products without the need for physical contact or manipulation of the products, which can be especially useful in certain retail environments, such as those with fragile or perishable goods. Approaches for product detection with computer vision are reviewed in this study [11]. Shi et al. developed a smart library book sorting application with computer vision and barcode identification algorithms [12].

However, computer vision does have limitations [13, 14]. One key limitation of computer vision is its reliance on visual data. This means that it can struggle in situations where there is low light or other factors that make it difficult to capture clear images. Additionally, computer vision systems may struggle to accurately interpret

depth information, which can limit their ability to perform certain tasks. Figure 2-2 shows one of the limitations that computer vision might have when applied to the top of the shelf. The camera is the ZED 2 stereo camera from Stereolabs. Pasta boxes have been divided into three piles, with the number of layers increasing from one to three (corresponding to an increase in the total number of objects from 3 to 9), there was no significant difference in their appearance from the camera's perspective (especially for the middle stack) Figure 2-3. Another limitation can be observed when attempting material classification using a top-down camera view Figure 2-4.

Figure 2-2: Placement of Zed 2 camera above the tested area

The use of AIoT, or artificial intelligence over the Internet of Things, has become an inevitable trend in the development of RFID technology. For instance, Li et al. [15] proposes a novel hybrid system that integrates computer vision and RFID technology to recover the relative motion paths of RFID tags attached to individuals, and then establishes correlations between these paths and the physical motion paths of the individuals, which are captured using a 3D depth camera. Hsiao et al. [16] propose a new sensor deployment method for improving passive RFID localization accuracy. Duan et al. [17] present a system that combines both technologies to achieve precise localization and tracking of tagged objects .

Other artificial intelligence technologies are also being used to analyze the data collected by smart shelves and provide retailers with insights into customer behavior


Figure 2-3: Camera view when pasta boxes are stacked from 1 to 3

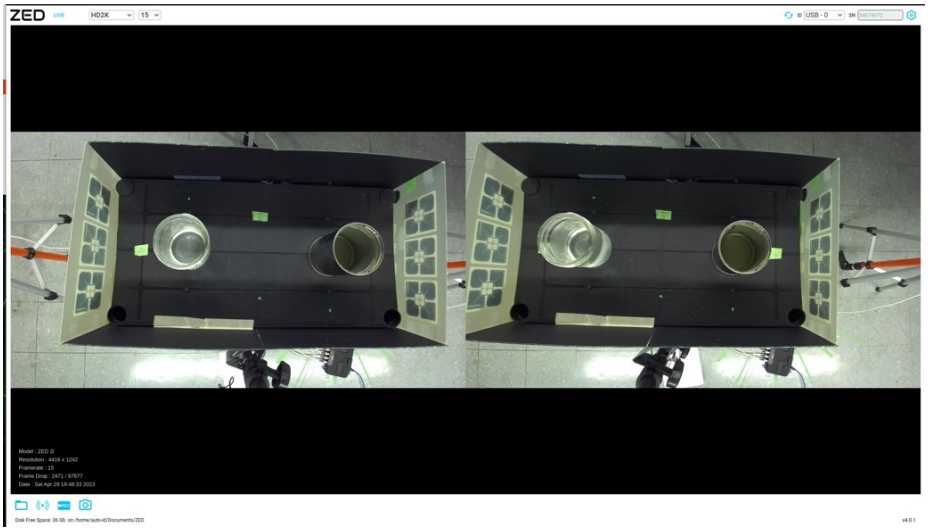


Figure 2-4: Camera view when one metal can (right) and one glass can (left) are put in the area

and preferences. Equipped with multiple sensors and cameras to track customer behavior, smart shelves can provide real-time recommendations and promotions based on a customer's preferences and purchasing history [18, 19].

The purpose of this thesis is to use RFID technology to assist smart shelf systems by providing context awareness. Three aspects ("real-time merchandise tracking", "stocks tracking" and "material classification") are focused. These three applications are not only practical but also provide more possibilities and feasibility for future omni-channel strategies.

### 2.2.1 Real-time merchandise tracking

Real-time tracking of merchandise has become an important aspect of retail management. It enables monitoring of the location and movement of products in real time. The purpose is to improve supply chain efficiency, prevent losses due to theft or misplacement, and increase customer satisfaction by providing accurate information about the availability of products.

Historically, real-time tracking in retail was accomplished using barcode scanning and handheld devices [20]. Afterward, the use of RFID allows for the automated tracking of products in real-time without the need for manual scanning. Initially,

tags that can be read by RFID readers are attached to products, providing real time information about their location and movement. However, this requires every single item to be tagged, which can be a time-consuming and expensive process, especially for large inventories. Additionally, the cost of RFID tags can add up quickly, further increasing the expense of implementing a real-time tracking system.

### 2.2.2 Stocks tracking

While merchandise tracking refers to the process of monitoring individual products from their arrival in the store until they are sold, stock tracking involves monitoring the number of products available in stock. Both processes are essential for retailers to ensure that they have sufficient inventory to meet customer demand and to minimize the risk of overstocking or stock-outs.

Stock tracking helps retailers to optimize their inventory management by providing real-time data on stock levels, which can help retailers or companies identify trends in product sales, enabling them to adjust their product offerings or promotional strategies accordingly. It also leads to an essential component of inventory management in various industries, from retail to manufacturing- auto-restock. Auto-restock refers to the process of automatically replenishing stock levels when they fall below a certain threshold. By automating the restocking process, companies can reduce the time and resources required to manually monitor and order inventory, and ensure that stock levels are always maintained at optimal levels. One of the most common solutions is the use of an inventory management system with automated replenishment capabilities [21, 22]. With automated replenishment, the inventory management system is integrated with the supplier's system, and when inventory levels reach a certain threshold, the system automatically generates a purchase order for replenishment. This technology can reduce manual errors and ensure that stock levels are always optimized.

On the hardware side, similar to merchandise tracking, barcodes, and RFID are widely applied for auto-restock by tracking their movement in and out of the inventory while they have similar limitations as mentioned in 2.2.1.

### 2.2.3 Material classification

Material classification refers to the process of categorizing products based on their material properties, such as plastic, metal, or glass. It helps in supply chain management, allowing businesses to track their inventory, monitor production, and improve overall efficiency. Firstly, material classification helps retailers to reduce waste by enabling them to better track and manage products that are close to or past their expiration date. By categorizing products by material, retailers can quickly identify which products are most likely to expire and take action to prevent waste, such as discounting or donating the products before they expire.

Secondly, material classification enables retailers to implement sustainable practices. By tracking the number of items made from each material type, retailers can identify which materials they are using most and prioritize sustainable alternatives. For instance, if a retailer discovers that they use a significant number of plastic items, they can consider switching to biodegradable materials such as paper or plant-based plastics. This can further help retailers reduce their environmental impact and improve their brand image.

Thirdly, material classification can improve the efficiency of the supply chain [23]. By identifying the material type of each item, retailers can streamline their sorting and stocking processes. This efficiency can reduce the time and labor required for inventory management, allowing retailers to allocate their resources more effectively. In reality, products made of glass may require specialized handling and transportation to prevent breakage, while products made of plastic may be more resilient and require less care during transport.

Several technologies and applications have been developed to enable material classification, including RFID, computer vision, and machine learning algorithms [24, 25, 26]. A camera can capture images of products on a shelf, and machine learning algorithms can be used to classify the products based on their shape, color, and other visual properties.

The promising advantages of material classification in retailers are numerous. Ad-

ditionally, by better understanding the types of products they carry and their corresponding material properties, retailers can create targeted marketing campaigns and product displays that appeal to specific customer segments, further increasing customer satisfaction and loyalty.

# Chapter 3

# Existing related research work

In this section, the state-of-the-art of UHF RFID being applied to do localization and sensing works are to be briefly introduced.

## 3.1 UHF RFID localization

While being used for localization, UHF RFID is able to provide location information without requiring line-of-sight or direct physical contact with the tags. This makes it suitable for applications where traditional localization technologies, such as Global Positioning System (GPS), may not be feasible or effective, especially in indoor environments or areas with obstructions.

Other localization technologies include infrared, ultrasonic, wireless local area network (WLAN), Bluetooth, Ultra-Wide Band, ZigBee, etc. However, they are more or less constrained by short range, high construction cost, limited energy consumption, limited coverage area, poor real-time performance, or the need for line-of-sight (LOS) [27].

In terms of the localization principle, current methods can be categorized into two types: range-based and range-free. Range-based localization methods are widely employed in traditional positioning applications. By analyzing as Received Signal Strength Indicator (RSSI), Time of Arrival (TOA), Time Difference of Arrival (TDOA), or phase of the RFID signals, it is possible to estimate the location of the

tagged objects based on geometric relationships [28, 29, 30, 31, 32]. Although range-based localization methods have a simple principle, they suffer from drawbacks such as low accuracy, extensive computational requirements, and sensitivity to complex environmental conditions.

On the other hand, range-free methods rely on scene analysis, where environmental parameters are quantified to create an information map specific to the localization scenario. This approach can be classified further as fingerprinting and non-fingerprinting methods. In fingerprinting, there are two phases: the online phase (Real-time phase) and the offline phase (Training phase). In the offline phase, RSS regarding location is measured and stored in a database, while in the online phase, the tested location estimation is gained by comparing RSS measurements with the database. For non-fingerprinting, an approach known as Radio Tomographic Imaging (RTI) [33] has been studied, which utilizes RSSI information to create images of signal attenuation in the environment. This approach holds promise for applications such as mobile human positioning and through-wall localization and is the approach this thesis applies.

## 3.2 UHF RFID sensing

UHF RFID sensors provide high accuracy and reliability in data collection, enabling precise and consistent measurements. They exhibit a wide sensing range and can operate in harsh environments, making them suitable for various applications, as [34, 35, 36, 37] presented.

Previous studies have focused on establishing a correlation between the analog response of the tag and a sensor integrated into its antenna structure. This sensor component can cause impedance mismatch at the antenna-chip interface, leading to modifications in transmitted power. To directly process analog measurements and digitally transmit the information to the reader, RFID tags are designed to be equipped with built-in Analog-to-Digital converters [38]. This reduces the impact of disturbance introduced by the wireless link between the reader and the tag. Being compatible with EPC Gen 2, the tags could be integrated with other functions, to

establish a complete sensing system [39].

This thesis has a part of battery-free environmental sensing, with EPC compatible tags, to add values to the context awareness system. Furthermore, this work also provides possibilities for a sensor platform that enables large-scale integration of sensors and utilizes real-time data for decision-making and control.

# Chapter 4

# Basics of RFID technology

In this thesis, UHF RFID serves as the foundation of the entire system. The tag's response, Received Signal Strength (RSS), is used for a series of calculations and analyses to provide an estimation of the objects' quantities, materials, and positions on a smart shelf. The following sections will introduce the basic principles of RFID, the generation of signals, and the communication process of the RFID system. For explaining the sensing platform, the Class 1 Gen 2 protocol is also introduced.

## 4.1 History of RFID

Radio Frequency Identification (RFID) is a wireless technology that has been used in various applications such as supply chain management, inventory control, and asset tracking.

The concept of RFID dates back to World War II when British engineers used a radar system to identify their own planes from the enemy planes, by changing attitude and thus changing the signal backscattered to radar.

Later in the 1970s, works are aiming at electronic toll collection, animal and vehicle tracking, and factory automation. RFID technology has then been extensively deployed, finding widespread utilization in various domains.

Presently, numerous organizations worldwide, including prominent retail chains, employ RFID tags for diverse purposes such as asset tracking, inventory management,

and quality control procedures. Enabled by technological advancements, these tags have the capability to monitor a wide range of items.

## 4.2 Types of RFID

There are three types of RFID tags: passive, active, and semi-passive. Tags could also be differentiated by frequency range (low, high, and ultra-high)

Active tags, possess their own power source and transmitter enabling the tag to broadcast its signal, tend to be significantly more costly and are typically reserved for the tracking of exceptionally valuable assets, such as equipment within the construction, automotive, or healthcare sectors.

Passive RFID tags do not have a built-in power source but instead rely on the electromagnetic energy from the reader to power the tag and transmit data. Passive RFID tags are smaller and less expensive than active tags, making them well-suited for applications where cost and size are important factors. However, passive tags have a shorter read range than active tags and are less reliable in environments with high levels of interference.

Semi-passive RFID tags, also referred to as battery-assisted tags, are equipped with an internal battery but differ from active RFID tags as they do not transmit periodic signals. Instead, the battery is solely utilized to activate the tag upon receiving a signal, allowing the entirety of the reader's energy to be reflected back.

## 4.3 Radio basics of UHF RFID

### 4.3.1 UHF RFID and its current applications

UHF RFID tags and readers commonly function within the frequency range of 860-960 MHz. Compared to low-frequency (LF) and high-frequency (HF) tags, UHF RFID tags have a faster data transfer rate and offer significantly extended read ranges up to 50 feet. Their ability to rapidly transfer data makes them particularly suitable for applications necessitating simultaneous reading of multiple items, such as boxes

of merchandise passing through a warehouse entrance. The use of UHF technology spans many markets; including retail, healthcare, life science, pharmaceutical, anti-counterfeiting, transportation, and manufacturing. Some of the common use cases of UHF RFID are:

**Logistics and Supply Chain Management:**

One of the primary applications of UHF RFID is in logistics and supply chain management. UHF RFID enables real-time tracking of inventory and assets, which can help companies improve efficiency, reduce costs, and optimize their supply chain operations.

**Retail:**

By using UHF RFID tags on products, retailers can track inventory levels in real time, reducing the likelihood of stockouts and overstocks. UHF RFID can also help retailers improve their omnichannel capabilities, by enabling them to track products across different channels and locations.

**Healthcare:**

UHF RFID can be used to track patients and monitor their movements throughout a healthcare facility, ensuring that they receive the appropriate care and treatment [40]. UHF RFID can also be used to track medical equipment and supplies, reducing the likelihood of loss or theft.

### 4.3.2 Radio Basics

#### Electromagnetic Waves

RFID technology uses electromagnetic waves to communicate between the reader and the tag. According to Daniel Dobkin's book, "The RF in RFID" [41], an antenna is a device to produce currents and charges whose effects don't cancel for a distant observer. The emission of electromagnetic waves from a transmitting antenna induces a voltage in a receiving antenna.

### Modulation

RFID technology uses modulation techniques to encode data on electromagnetic waves. The reader sends a signal to the tag with a specific frequency, and the tag responds by modulating the reflected signal with its own data. During modulation, the carrier frequency is multiplied by a slowly varying signal, which is known as the baseband information, thus spectrum becomes wider. RFID signals or symbols, are digitally modulated to carry a binary "0" and "1".

For instance, pulse-interval encoding (PIE) is a coding technique that involves encoding the binary data before modulation. In PIE, a binary '1' is represented by a brief power-off pulse following a prolonged full-power interval, while a binary '0' is represented by a shorter full-power interval accompanied by the same power-off pulse (Figure 4-1). The resulting encoded baseband signal is subsequently employed for modulating the carrier signal.

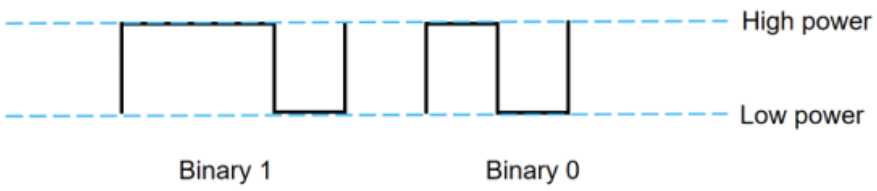


Figure 4-1: Pulse-interval encoding

### Backscatter Radio Links

RFID tags use backscatter radio links to communicate with the reader. To transmit information to the reader, the RFID tag modulates the backscattered signal. Start with transmit antenna current, if there is a load existing in receive antenna, a current will be induced. The induced current can then generate radiated waves back. However, if the load in receive antenna is not enough for transferring induced voltage to current, there will be no backscattered (Figure 4-2).

Methods to encode the signal from RFID tags are based on quantifying the number of transitions in the tag's state within a specific time frame. Alternatively, these

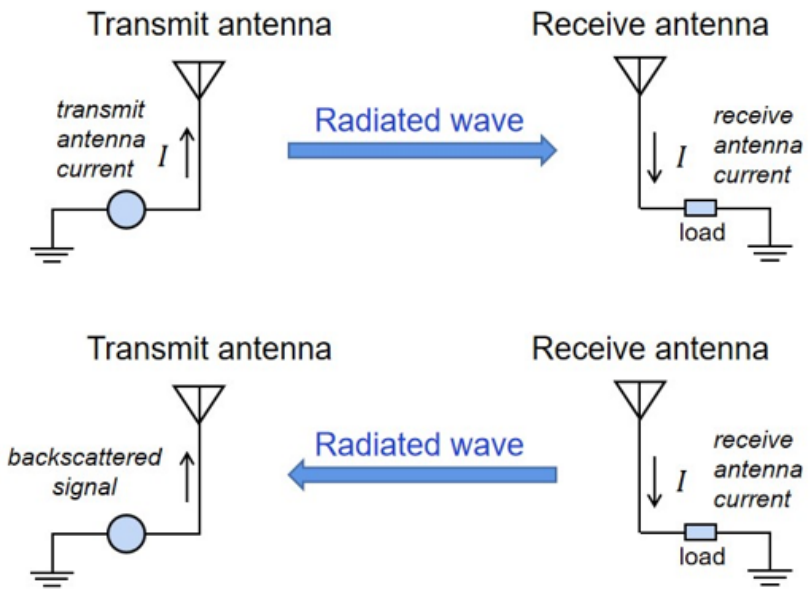


Figure 4-2: Backscattered link

methods involve manipulating the frequency of the tag's state transitions. Thus, all tag codes utilized in RFID systems are variations of frequency-shift keying (FSK). It is important to emphasize that the frequency referred to in this context does not pertain to the radio carrier frequency, such as 900 MHz, but rather the tag's baseband frequency, typically around 100 or 200 kHz. For instance, a binary '1' could be encoded by a tag to transition its state 100 times per millisecond, while a binary '0' might entail 50 state transitions per millisecond. This is also called subcarrier modulation as the frequency being altered is the frequency at which a carrier wave is modulated in amplitude.

### Tags' response signal

The reader evaluates the tag's response and delivers the tag's data alongside the Received Signal Strength Indicator (RSSI). RSSI is a metric that quantifies the power received from the reflected signal of an RFID tag when queried by a reader. It essentially denotes the power level of the tag's backscattered response signal in relation to the power level of the reader's initial transmission signal. RSSI values serve to

provide a general assessment of the tag's responsiveness within a read zone. When comparing different tags, RSSI can offer valuable insights into their performance within a similar environment. However, it is important to note that RSSI values do not provide an accurate measure of the tag's distance from the antenna in a passive RFID system.

In addition to RSSI, the majority of RFID readers enable the measurement of both the power and phase of the tag signal. By combining both phase and RSSI information, some applications have been developed to do localizations or other tracking jobs [42, 43].

### RFID protocols

RFID protocols are the set of rules that govern how RFID tags and readers communicate with each other.

#### EPCglobal Generation 1 Class 0 (G1C0)

EPCglobal G1C0 laid the initial groundwork for the development of standardized RFID protocols. The Class 0 classification initially referred to tags that were factory-programmed as read-only. The use of Electronic Product Codes (EPC) with both 64-bit and 96-bit lengths was envisioned and has been commercially implemented. Read symbols for Class0 are pulse-length-encoded and amplitude-shift-keyed, while tag symbols are defined by the frequency of transitions of the tag between different scattering states. Furthermore, the communication protocol between the tag and reader is structured to occur in a bit-by-bit query-response format, as opposed to a traditional packet transmission followed by a tag response. As a result, the integrated circuit within the tag can be designed to decode the reader bit and determine its response immediately after the gap, thereby facilitating modulation during the final portion of the reader symbols.

As the Class 0 protocol documentation characterized Class 0 tags as being pre-written at the factory, no mechanism for writing new data to the tags was established. Despite this, the need to write EPC to tags frequently arises in practice. Consequently, field-writeable tags were developed. Given that the standard document did

not specify the memory organization or commands required for such tags, different vendors resorted to disparate and incompatible approaches.

**EPCglobal Generation 1 Class1 (G1C1):**

Class 1 tags are considered passive tags, capable of backscattering a distinct ID to a reader. This classification assumes that tags can be reprogrammed at least once. Tags featuring EPC of both 64-bit and 96-bit lengths have been commercially introduced. Vendors such as Alien Technologies have sold significant numbers of Class 1 tags.

ClG1's reader symbol is also pulse-duration-encoded amplitude-shift-keyed, and tag symbols are frequently-shift-keyed (the number of state transmissions is different for binary '0' and '1'). Tags are equipped with security measures and support LOCK and KILL commands. The KILL command, which is shielded by an 8-bit password, features a timeout period following a KILL attempt aimed at preventing dictionary attacks on this vulnerable key. However, the timeout period is inadequate protection, and Class 1 tags cannot be considered secure against KILL attacks. In contrast to Class 0, the Class 1 protocol employs a reasonably traditional packetized half-duplex protocol in which the reader forwards a complete command packet, and the tags transmit a complete reply.

**ISO 18000-6C (EPCglobal Class 1 Generation 2):**

In 2004, EPCglobal introduced a new standard called Class 1 Generation 2 (Gen 2), which was later adopted as ISO 18000-6C. This standard aimed to address the limitations of Gen 1 by providing a longer read range, faster data transfer rates, and enhanced security features. Gen2 operates in the 860-960 MHz frequency range. It also incorporates anti-collision features, allowing multiple tags to be read simultaneously, and provides support for encryption and authentication.

Compared to previous protocols, Gen2 has enhancements such as flexible tag data rates, spectral control of reader and tag transmissions, variable-length commands for inventory speed improvements, and explicit specification of memory maps.

**Tag memory organization**

Gen 2 tags have a memory with two obligatory banks and two optional memory

banks. They are numbered in binary: Figure "00" is the Reserved bank which contains the 32-bit KILL and ACCESS passwords;

"01" is the EPC bank which includes 32-bit Protocol Control word, EPC as well as CRC16 for error checking;

"10" is the Tag ID bank which contains identifying information;

"11" is the User bank that is available for any application-specific data. It is a rewritable memory area and is typically used to store information specific to the application for which the tag is being used. The user memory bank can be accessed and modified by authorized parties using RFID readers with appropriate permissions.

**Reader and tag symbols**

Reader symbols in Gen2 are amplitude-modulated and pulse-interval-encoded (PIE). The binary '0' in the PIE system is represented by a power-on interval followed by an equally long power-off interval. The length of the binary '0' symbol, referred to as Tari, determines the total duration of the symbol. The pulsewidth PW is defined as half of Tari. A binary '1' symbol, with a total duration ranging from 1.5 to 2 Tari, has the same pulsewidth as '0' but an extended power-on interval. The standard Tari values are 6.25, 12.5, and 25 microseconds, which correspond to symbol rates of 160, 80, and 40 kbps (Figure 4-3).

When multiple readers are operating in the same area, interference can occur, leading to reduced read range or even failure to read the tag. To mitigate these issues, different operating categories for RFID readers have been defined, each with corresponding limitations on the transmitted spectral width. The first operation involves a single interrogator and requires the reader transmission to comply with the regulations set by the relevant authority. This category is suitable for situations where only one reader is present in the area.

The second operation is intended for cases where multiple interrogators are present in close proximity, and the number of readers is relatively small compared to the number of channels available. In this category, the reader transmission is constrained to minimize interference in adjacent or second-adjacent channels.

The third operation, known as Dense Interrogator operation, is designed to ensure

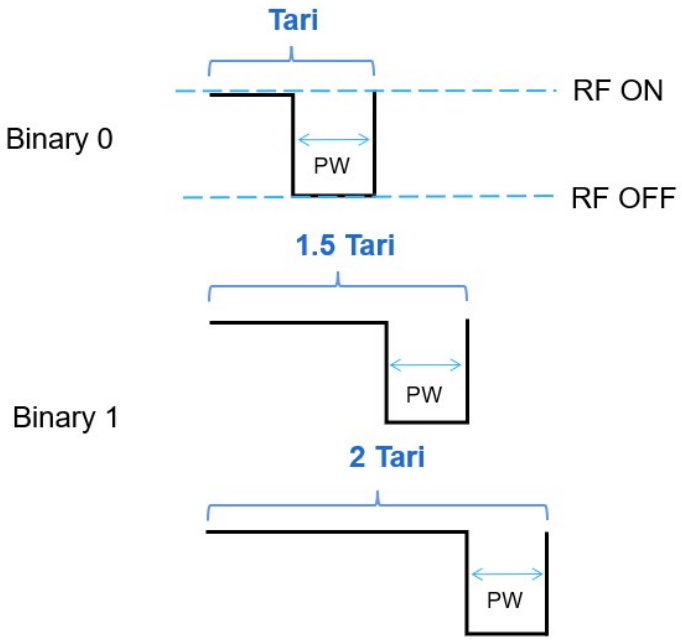


Figure 4-3: Reader symbols

successful tag reading even when all available channels are being used by a reader transmitter. In this category, the transmitted spectrum width is tightly controlled to prevent interference between readers. This category is suitable for high-density reader environments, such as in warehouse or distribution center settings.

For tag symbols, the default operating mode (FM0) and Miller-modulated subcarrier (MMS) encoding are defined in Gen2. In FM0, a binary "0" and "1" has the same symbol time (denoted as Tpri), while "0" has an additional state transition in the middle. In terms of implementation, FM0 signaling is straightforward and has a bit rate of 1 per symbol time. However, its successful operation relies on the precise detection of a single transition to differentiate between data bits. Additionally, the signal spectrum of the tag is not optimal for preventing interference from co-channel readers.

MMS is aiming to offer greater flexibility in balancing the tradeoff between noise and data rate and managing the spectrum. In MMS, transition ways of binary "0" and "1" are exchanged (baseband coding), and there is no state transition at the symbol edges between consecutive 1s, or between a 1 and a 0. Then the baseband coding is

subjected to multiplication using a square wave, which comprises M cycles in each baseband symbol. As a consequence, the resulting signal exhibits a square wave-like pattern and experiences periodic phase inversions. With a larger M number, more cycles are needed to transmit one binary symbol. Thus, the rate of transmission of data is reduced but the spectrum turns to be narrower. MMS enables improved spectral efficiency and lower power consumption.

**States and commands**

Medium access control is followed by Q protocol or slotted Aloha variant, by which a numerical parameter Q is contained in Query command. In Gen2, tags have multiple states such as "Ready", "Arbitrate", "Reply", "Acknowledged", "Open", "Secured" and "Killed", transitioning between each other according to Query command and the tag's response. There are commonly applied commands for users such as "Read", "Write", "Lock" and "Kill".

Read command can read from any memory area that is not locked against reading. Parameters for read commands are:

- Memory Bank: specifies whether the Read command accesses Reserved, EPC, TID, or User memory.
- Word Pointer: specifies the starting word address inside Memory Bank, where words are 16 bits in length.
- WordCount: specifies the number of 16-bit words to be read.
- RN: handle of the tag to be read
- CRC16: error check on the command.

Writing syntax is very similar to that of Read, except that the WordCount is replaced by the 16 bits of cover-coded data to be written.

Overall, Gen 2 represents a significant improvement over previous generations of RFID technology and has been widely adopted in a range of applications. Gen 2 tags also include memory that can be read and written to, allowing for additional data

to be stored on the tag, such as production date, batch number, or other relevant information.

# Chapter 5

# Methodologies and experiment design

## 5.1 RTI mechanism

### Introduction

Radio tomography imaging (RTI) [33] is a non-invasive remote sensing technique that has gained significant attention in recent years due to its unique advantages, such as its ability to operate in harsh environments, penetrate obstacles, and provide continuous, real-time monitoring. Moreover, with the advancements in wireless communication technologies, the increasing availability of low-cost radio transceivers, and the development of sophisticated signal processing techniques together with machine learning algorithms, RTI has become a practical and cost-effective solution for imaging and monitoring objects or environments using radio frequency signals.

### Fading

Fading is a phenomenon in radio frequency communication that results in the attenuation (reduction of signal strength) or distortion of a transmitted signal as it propagates wirelessly. This can lead to reduced signal strength, increased noise and errors, degraded overall system performance or even short failure of communication. Fading could occur due to a variety of factors, including the physical characteristics of the wireless channel, interference from other RF sources, and environmental factors

such as atmospheric conditions. In general, fading is caused by the fact that radio waves travel through space and encounter obstacles and reflections that cause them to scatter and interfere with each other.

There are two main types of fading: path loss and multipath fading. Path loss occurs when a signal is attenuated as it travels through space due to distances, the presence of obstacles, or atmospheric absorption. Multipath fading occurs when transmitted signals encounter multiple reflectors in the environment during their propagation, resulting in constructive and destructive interference that can cause fluctuations in the received signal strength.

RTI works by utilizing the attenuation and scattering effects of radio waves as they propagate through a region of interest. As the signals propagate through the region, they are attenuated by any objects present, causing fluctuations in the received signal strength. By analyzing these fluctuations, RTI algorithms can reconstruct an image of the object or objects within the region, which can also provide valuable insights into the underlying physical properties of the medium.

The use of attenuation in RTI is particularly useful because it enables imaging of objects that are otherwise difficult or impossible with other wireless techniques. For example, RTI can be used to track people or objects behind walls or other obstacles, making it useful for applications such as security and surveillance. However, it's important to note that attenuation can also present challenges for RTI, particularly in environments with high levels of multipath (many reflective surfaces) or other interference. In these cases, sophisticated algorithms and signal processing techniques are needed to extract useful information from the attenuated signals.

### Model of RTI

Within the linear model by Joey Wilson and Neal Patwari [33], for K nodes in the RTI network Figure 5-1, $M = \frac{K^2-K}{2}$ unique links (one node to another) exist. The signal strength $y_i(t)$ of a particular link i at time t can be expressed as:

$$y_i(t) = P_i - L_i - S_i(t) - F_i(t) - v_i(t) \tag{5.1}$$

where:

- $P_i$: Transmitted power in decibels.
- $S_i(t)$: Shadowing loss in decibels due to objects that attenuate the signal.
- $F_i(t)$: Fading loss in decibels that occurs from constructive and destructive interference of narrow-band signals in multipath environments.
- $L_i$: Static losses in decibels due to distance, antenna patterns, device inconsistencies, etc.
- $v_i(t)$: Measurement noise

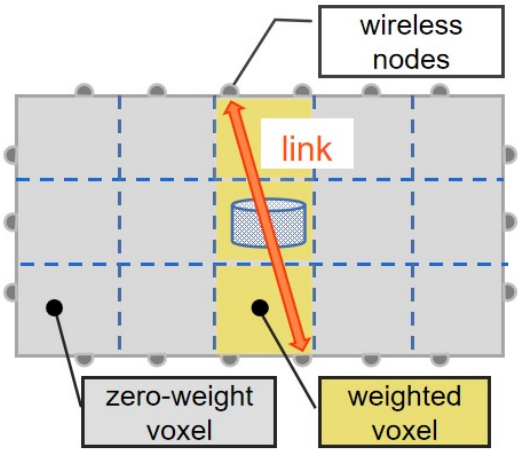


Figure 5-1: Illustration of RTI network. Radio links are between wireless nodes and weights could be distributed to each voxel in the tested region.

The shadowing loss $S_i(t)$ can be estimated by summing up the attenuation that happens in each voxel. A weighting factor is employed because the contribution of each voxel to the attenuation of a specific link varies. Mathematically,

$$S_i(t) = \sum_{j=1}^{N} w_{ij} x_j(t) \tag{5.2}$$

$x_j(t)$ is the attenuation occurring in voxel j at time t, and $w_{ij}$ is the weighting of pixel j for link i. If a link does not pass through a specific voxel, that voxel is excluded

from consideration by assigning a weight of zero. It is worth mentioning that voxels are in three-dimensional space where attenuations truly happen, while pixels are in two-dimensional space where the image is generated. Thus, RTI provides a mapping from three-dimensional to two-dimensional space, by imaging attenuations to each pixel in the region.

By considering the difference of signal strength at two time points, and all static losses can be cancelled after subtraction, the change in RSS could be expressed as:

$$\Delta y_i = y_i(t_b) - y_i(t_a) = S_i(t_b) - S_i(t_a) + F_i(t_b) - F_i(t_a) + v_i(t_b) - v_i(t_a) \quad (5.3)$$

With Eq. 5.3, this can also be expressed as:

$$\Delta y_i = \sum_{j=1}^{N} w_{ij} \Delta x_j + n_i \quad (5.4)$$

Where $n_i$ is the noise from fading and measurement noise $F_i(t_b) - F_i(t_a) + v_i(t_b) - v_i(t_a)$ and $\Delta x_j = x_j(t_b) - x_j(t_a)$ is the difference in attenuation at voxel $j$ from time $t_a$ to $t_b$.

In matrix form, the system (with $M$ links and $N$ voxels in total) can be interpreted as:

$$\Delta y = W \Delta x + n \quad (5.5)$$

where:

$$\Delta y = [\Delta y_1, \Delta y_2, \ldots, \Delta y_M]^T \quad (5.6)$$

$$\Delta x = [\Delta x_1, \Delta x_2, \ldots, \Delta x_M]^T \quad (5.7)$$

$$n = [n_1, n_2, \ldots, n_M]^T \quad (5.8)$$

$$[W]_{i,j} = w_{i,j} \tag{5.9}$$

In summary, $\Delta y$ denotes the difference of RSS measurements in all links, n interprets the noise for all links, and $\Delta x$ is the attenuation which is used to generate maps, W is the weighting matrix of dimension M×N, for each row, weights for every pixel of that particular link are included. All variables are measured in decibels (dB) but in this thesis, signals are in decibels per milliwatt (dBm).

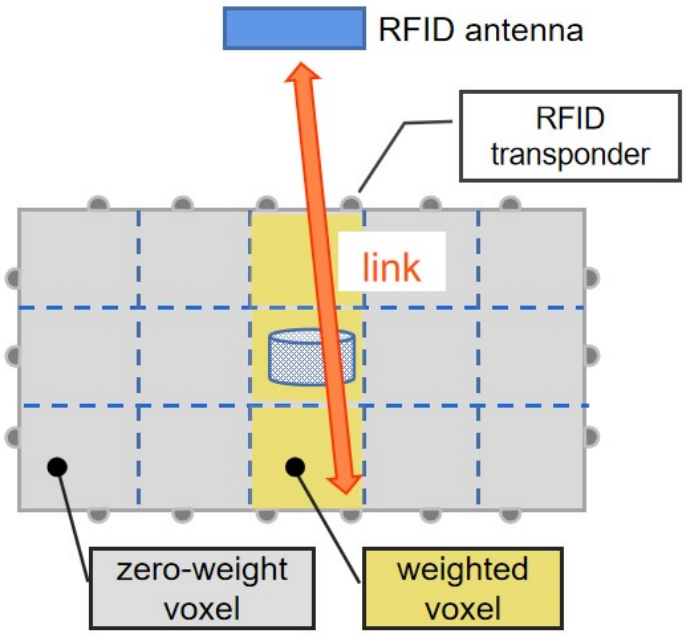


Figure 5-2: pRFID based RTI network where links are between antenna and RFID transponders.

In 2012, Benjamin et al. [44] applied RTI in device-free user localization, using passive RFID (pRFID) field communication, containing transmitters/transponders and receivers/antennas Figure 5-2. Forward link from transponder and reverse link from the transponder back to reader are defined, and multiple voxels are uniformly segmented from a target region. A bistatic weighting model is also defined to differentiate forward and backward links, since an object might generate different attenuations regarding to power difference. This work is a new approach to do device-free

indoor user localization with passive RFID.

## 5.2 Weight model

The weight matrix generally describes the influence from physical objects on paths' signal strength. According to study by Patwari et al. [45], one method for determining the weighting of each link in the network is to employ an ellipsoid with foci at the locations of each node. Voxels that fall outside the ellipsoid are assigned a weight of zero, while voxels that lie within the line of sight (LOS) path determined by the ellipsoid are weighted inversely proportional to the square root of the link distance. This weighting scheme takes into account the intuition that longer links provide less information about the attenuation in voxels they traverse.

The weight model can be described mathematically as:

$$w_{ij} = \frac{1}{\sqrt{d}} \begin{cases} 1, \text{if } d_{ij}(1) + d_{ij}(2) < d + \lambda \\ 0, \text{otherwise} \end{cases} \tag{5.10}$$

Where d denotes the spatial separation between two specific nodes, $d_{ij}(1)$ and $d_{ij}(2)$ refer to the distances from the centroid of pixel j to the locations of the two nodes associated with link $i$. Meanwhile, the parameter $\lambda$ is a modifiable factor that characterizes the extent of the ellipse's width 5-3.

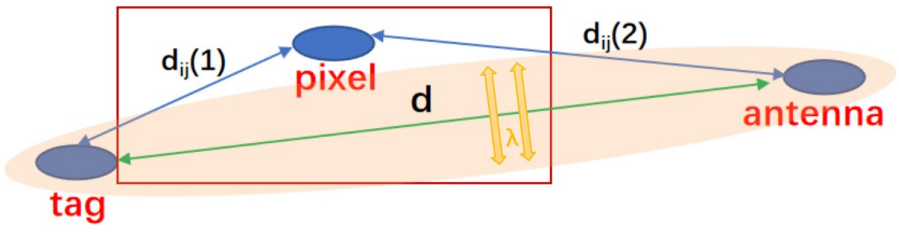


Figure 5-3: Illustration of weighting model

## 5.3 Regularization for ill-posed problems

The linear equation $y = Wx + n$ represents a fundamental model for characterizing the relationship between an input signal $x$ and an output signal $y$. The equation takes the form of a linear mapping between the input signal and the output signal, where W represents a matrix of coefficients that define the linear transformation and n represents additive noise that corrupts the output signal. This model is commonly used in applications such as data transmission, image processing, and audio processing, where the goal is to recover the original input signal from a noisy or distorted version of the signal. By estimating the values of the matrix W and the noise n, it is possible to develop effective algorithms for signal recovery and denoising, making the $y = Wx + n$ equation a powerful tool in the field of signal processing.

RTI has the form as well, in which y is the measured data and x is the desired attenuation matrix. One common solution is the least-squared-error method. Mathematically,

$$x_{LS} = \arg\min_{x} \|Wx - y\|_2^2 \tag{5.11}$$

The least-squares solution is a widely used method in statistical analysis and optimization for finding the best-fit parameters of a model that minimizes the sum of the squares of the residuals between the predicted values of the model and the actual observed values. The method is based on the principle of minimizing the sum of the squared residuals, which is equivalent to finding the maximum likelihood estimate of the parameters in a linear regression model. The least-squares solution can be applied to a wide range of problems, including curve fitting, regression analysis, and time series analysis, and is known for its simplicity and efficiency.

Letting the gradient of Eq. 5.11 to be zero, least square solution can be obtained:

$$
\begin{aligned}
&\partial(\arg\min_x \|Wx - y\|_2^2)/\partial x \\
&= \frac{\partial[(Wx-y)^T(Wx-y)]}{\partial x} \\
&= \frac{\partial(x^TW^TWx - y^TWx - x^TW^Ty + y^Ty)}{\partial x} \\
&= 2W^TWx - 2W^Ty
\end{aligned}
\tag{5.12}
$$

$$
x_{LS} = (W^TW)^{-1}W^Ty \tag{5.13}
$$

However, this solution is only valid when W is full-rank and is not suitable for ill-posed inverse problem, which is commonly the case RTI belongs to.

Ill-posed problem is firstly mentioned by Jacques Hadamard, saying that a problem is well-posed, if:

- it is solvable
- its solution is unique
- its solution depends continuously on system parameters, otherwise it is an ill-posed problem. The solution to an ill-posed problem is not unique or stable with respect to small perturbations in the data. The key to solve these problems is to find a stable and reliable solution with robustness to errors and noise in the data.

A powerful tool for the analysis of the least squares problem is the singular value decomposition (SVD). By doing SVD decomposition of weight matrix:

$$
W^{mxn} = U\Sigma V^T \tag{5.14}
$$

where $U^{m\times m}$ and $V^{n\times n}$ are orthogonal matrices and $\Sigma^{m\times n}$ is a rectangular diagonal matrix with non-negative real numbers on the diagonal. The columns of U and the columns of V are called left-singular vectors $u_1, u_2, \ldots, u_m$ and right-singular vectors $v_1, v_2, \ldots,\ v_n$ of $W$, respectively. The sorted diagonal entries of $\sigma_i$ are uniquely

determined by $W$ and are known as the singular values of $W$, and the number of non-zero singular values is equal to the rank $r$ of $W$.

The singular value decomposition can be written as:

$$W = \sum_{i=1}^{r} \sigma_i u_i v_i^T \tag{5.15}$$

$$x_{LS} = V\Sigma^{-1}U^T y = \sum_{i=1}^{N} \frac{1}{\sigma_i} u_i^T y \; v_i \tag{5.16}$$

From the above expression, the solution could be out-bounded with small singular values of $W$. In practice of RTI, small singular values in weight matrix $W$ lead to unstable results. For example, for a pixel arrangement of $5 \times 10$ in horizontal and vertical directions and 50 cm distance between antennas and tested area (refer to the later test setup chapter), the largest singular value of weight matrix is 1.55 while the last three smallest singular values are with order of magnitude of $10^{-16}$ and $10^{-17}$.

As one of the common solutions to deal with ill-posed question, the method involves adding a regularization term to the object function with a regularization hyperparameter $\alpha$:

$$f(x) = \frac{1}{2}\|WX - Y\|^2 + \alpha\|Qx\|^2 \tag{5.17}$$

By adding this term, the model is encouraged to find a balance between fitting the measured data and producing a smooth and more generalized image. The regularization term is typically in the form of the L2 norm of the image gradient, which effectively smooths the image and reduces noise. By taking derivative of Eq. 5.17, the solution could be calculated as

$$x_{LS} = (W^T W + \alpha \; Q^T Q \;)^{-1} W^T y \tag{5.18}$$

$Q$ is a matrix usually as a difference matrix evaluating the derivative operator [46]. For 2D plots, both derivatives in horizontal and vertical directions, $D_x$ and $D_y$, are applied, leading to

$$x_{LS} = [W^T W + \alpha(D_x^T D_x + D_y^T D_y)]^{-1} W^T y \tag{5.19}$$

Elements in $D_x$ and $D_y$ could be calculated by exponential spatial decay [47, 48]:

$$C_{m,n} = e^{\|p_m - p_n\|/\delta} \tag{5.20}$$

where $\delta$ is the correlation distance between pixel m and pixel n.

Truncated Singular Value Decomposition (TSVD) is another popular method used in data analysis and signal processing for dimensionality reduction and noise reduction. Based on SVD, TSVD involves only a subset of the largest singular values and their associated singular vectors, and discards the rest. This results in a low-rank matrix which is a compressed representation of the original matrix. TSVD is able to capture compressed representation of the received signal and thus has been shown to improve the accuracy of RTI image reconstruction by reducing noise and improving resolution. This method has pros as a computationally efficient solution to large-scale data problems. However, the main drawback of TSVD is that it requires a prior knowledge of the number of singular values and the noise level in the received signal, which can be a challenging task practically. Additionally, the truncation of singular values may lead to loss of information, which may affect the performance of downstream analysis. In this thesis, TSVD is not applied but might be explored in the future to get a comparison with Tikhonov Regularization method.

## 5.4 Test setup

Tests are done in an indoor room with experiment tables, digital displays, laboratory sink and electronic equipment such as DC supply, oscilloscope, digital multimeters, etc. The shelf is made up of plastic, and is placed in the central area of the room Figure 5-4.

The shelf region is a rectangular region with length of 60 cm and width of 32 cm. Three and six SMARTRAC Frog 3D RFID tags (18 tags in total) are attached

Figure 5-4: Test setting environment

to short and long sides, respectively. Four RFMAX S9028PCR antennas are placed around the shelf region, with a perpendicular distance of 50 cm to the shelf Figure 5-5. All RF signals are read through an Impinj Speedway R420 reader.

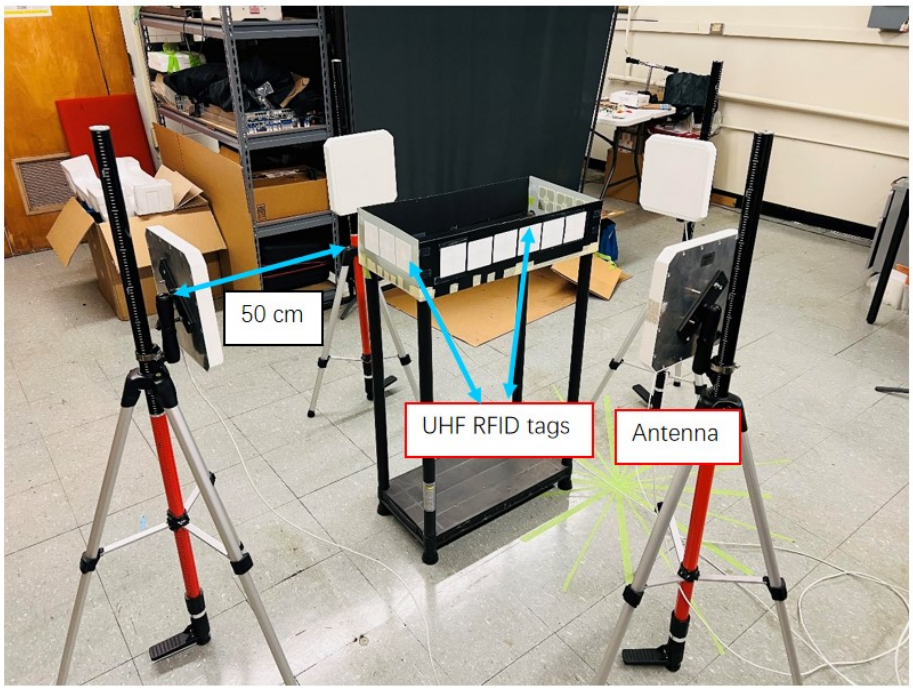


Figure 5-5: Placement of antennas and UHF RFID tags

## 5.5 Design problems

Studies have been done towards the numbers and placement of antennas. [44] Link density is defined as the total number of direct links (antennas to tags) in a single pixel. To get more intuitive thinking about relationship between RF paths and the particular pixel, we could use water reservoirs as an example Figure 5-6. Every link passed the pixel can be imagined as one water valve, whereas the weight corresponding to that link can be considered as open position of valve. The total volume of water in the reservoir is weighted sum of all sources. The larger link density of a pixel is, the easier for signal changes affect its attenuation. It is assumed that the probability of the object being placed in any given pixel is equal. Thus, in the design process, we strive for a uniform link density across the shelf, for detecting each possibility to

the maximum extent.

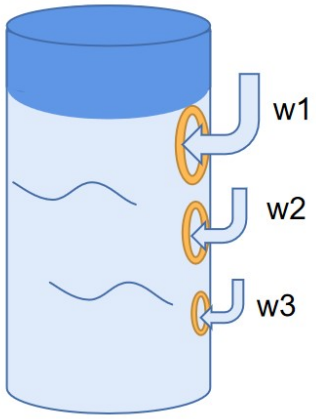


Figure 5-6: Each pixel could be thought as a water reservoir. Every link passing by could add a water valve to it, by which the open position of valve is controlled by weight assigned to that particular pixel.

With only two antennas, if they are placed in the diagonal direction facing each other, signals from all tags can be captured and added to heat map. However, links from antennas to tags might not be dense enough to cover the full region, thus precision and sensitivity of heat maps will be impacted. For the purpose of generating denser RF links, four antennas are applied to the experiments. The four antennas can be facing towards sidewalls (Setting 1) or diagonals (Setting 2) of the testing region Figure 5-7. The key consideration is to gain the largest transmission energy but not fall into short range region where the distance between the source and the observation point is small compared to the wavelength of the wave and wavefronts are curved. That is,

$$R > \frac{2D^2}{\lambda} \tag{5.21}$$

where R is the distance, D is the maximum linear dimension of an antenna, $\lambda$ is wavelength. To make sure no tag response is missing, a minimum distance of 50cm is quarantined between any antenna and its nearest tag. For each setting, all direct links are drawn and link density for every pixel is evaluated. For the rest of the part, setting 1 is chosen to collect data.

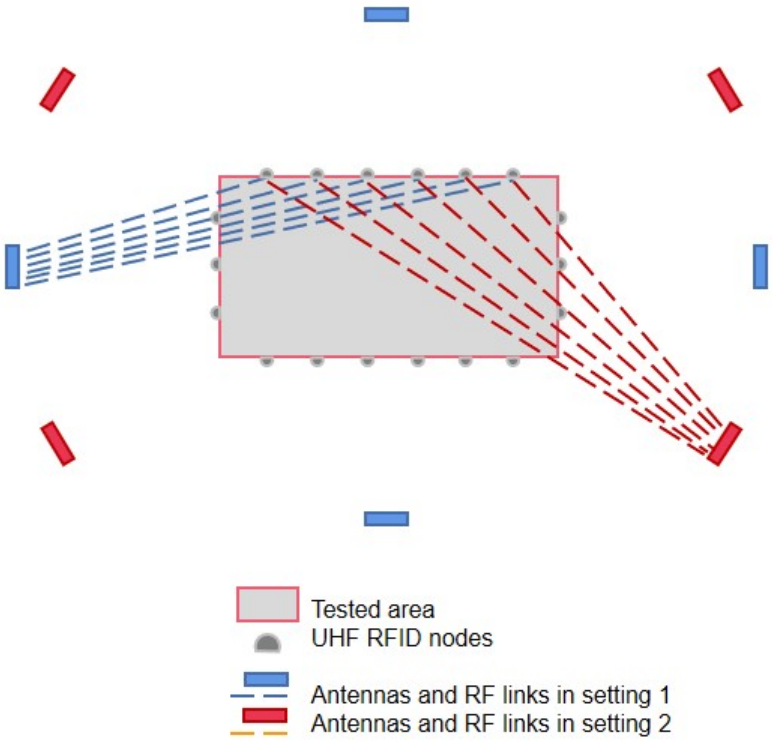


Figure 5-7: Two different placements of antennas

## 5.6 Measurement signal

Each measurement is made up of all four antennas reading 18 tags in the frequency range of 902.75 MHz - 925.25 MHz. All tests are done in Dual Target search mode, session 0 and maximum reader power and sensitivity. For measuring time of 1 min, around 3000 data points (Figure 5-8) can be measured for each antenna reading a single tag, spreading among frequency range. As a result, each frequency channel's RSSI value is the average value of all datapoints corresponding to that channel.

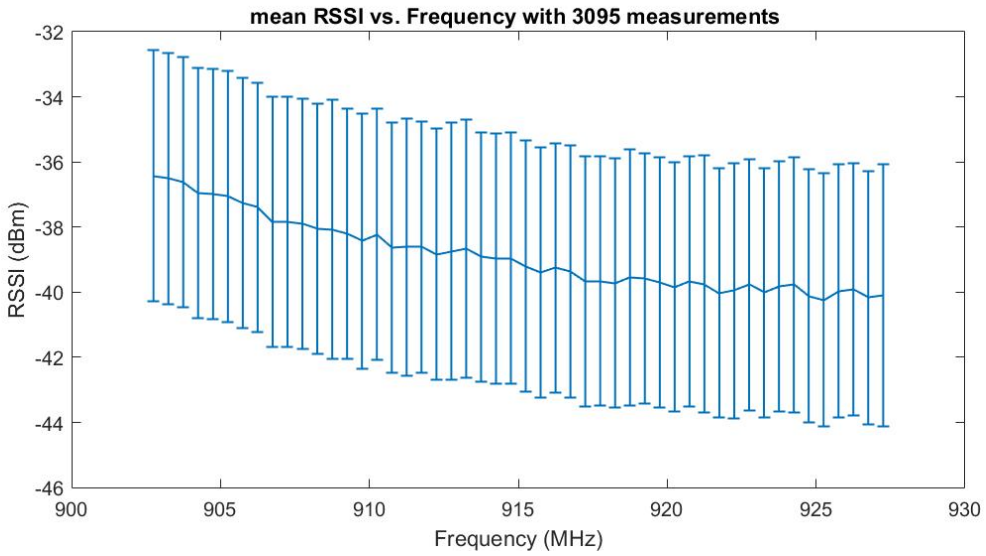


Figure 5-8: RSSI vs. frequency in 902.75 – 927.25 MHz of one antenna reading one tag

Since the RTI method takes advantage of "difference" in each RF link before and after an object's presence, there is always a calibration stage. In the experiment, RSSI values for all links are measured and stored when the shelf is empty (Stage 0). Then RSSI is measured after objects are placed on shelf (Stage 1) and difference values $\Delta RSSI$ between two stages are obtained. For every measurement, Stage 0 is measured once and used repeatedly, while in frequently-changing situation, recalibration is essential. Due to the construction and destruction interference effect, $\Delta$RSSI could have positive and negative values among different frequency channels, so the absolute value of the difference is taken, which is the original input data for further computation.

## 5.7 Parameter optimization

There are multiple parameters in the RTI model.

**- Correlation distance $\delta$**

In real life, direct RF link could have multi-path effect and the environment is full of reflections. This means that an object lay in one direct path might also bring attenuations to neighboring paths. In the expression of covariance matrix C, each element is defined as the covariance between two pixels using an exponential spatial decay, in which $\delta$ describes how significant are those effects.

**- Width of weighting ellipse $\lambda$**

In the weight matrix, whether a pixel has a weight to a particular link is determined by whether the corresponding voxel falls into the RF link region. $\lambda$ is the parameter describing the range of the ellipse region.

**- Number of channels taken into consideration n**

Since the measurements are done with dynamic activities going on, environment changing might influence signal differences between two phases. However, those changes might be small compared to those caused by object's existence. Some portion of channel data could be chosen to represent input data, with the aim to eliminating the influence of environmental factors. For the results shown, data from all channels are taken into account, this is due to the relative stable environment for most of the experiments.

**- Regularization parameter $\alpha$**

Within Tikhonov Regularization, a parameter $\alpha$ is to tune the effect of regularization.

To gain the range of each parameter, a prior test with two known positions has been down (Figure 5-9).

With the prior knowledge of two positions, accuracy can be calculated by averaging the Euclidean distances between real and estimated pixel center of position 1 and 2. Studies have been done on influences on localization accuracy when one parameter is altering and others are fixed.


Figure 5-9: Two prior positions for parameter optimization

| Parameter | Value |
|---|---|
| $\delta$ | 3 |
| $\lambda$ | 3 |
| $\alpha$ | 0.1 |
| n | 50 |

Table 5.1: The parameters to obtain the maximum accuracy of the two tested positions

The parameters to obtain the maximum accuracy of the two tested positions are summarized below (Table 5.1):

# Chapter 6

# Results

## 6.1 Location estimation without fingerprinting

Three positions are designed to be detected, which are on the upper left corner, middle right and bottom of shelf area Figure 6-1.


Figure 6-1: Illustration of three pre-defined positions

Measurements for each position are taken with four different objects (paper roll, olive oil bottle filled with oil, empty glass jar, empty plastic water bottle) Figure 6-2. Figure 6-3 shows that the real testing cases for three tested positions and Figure 6-4 shows position estimation results. The actual positions of the objects can be represented on heat maps as (1,1), (5,2), and (3,3) in the form of (horizontal position, vertical position).

Due to RF links effects caused by environments, such as multi-path and interference effects, the signal can be corrupted with noise and accuracy of the image will be


Figure 6-2: Objects whose location to be estimated

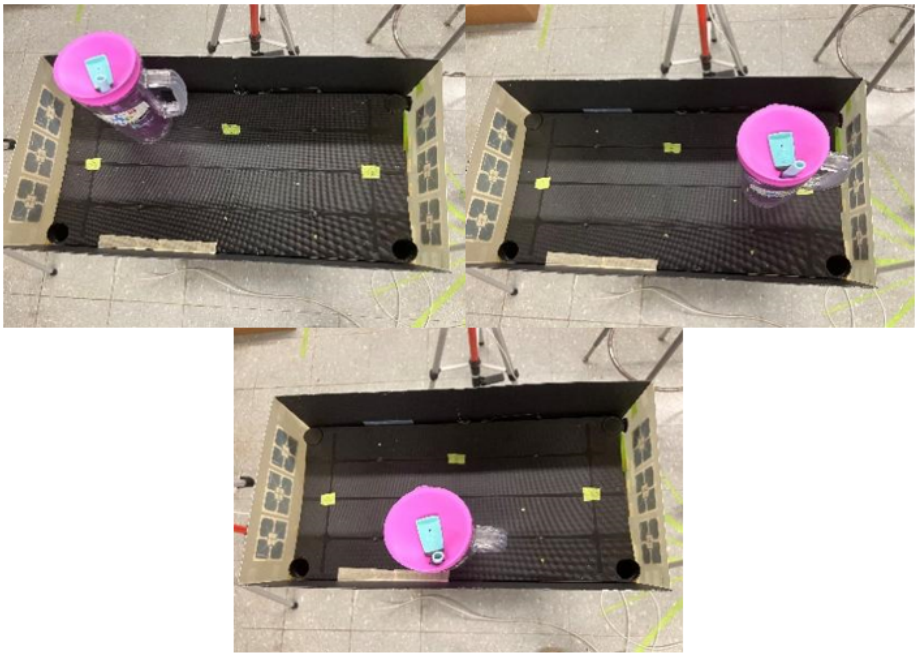

Figure 6-3: Real testing cases for three positions (left: 1, right: 2, bottom: 3 in Figure 6-1)

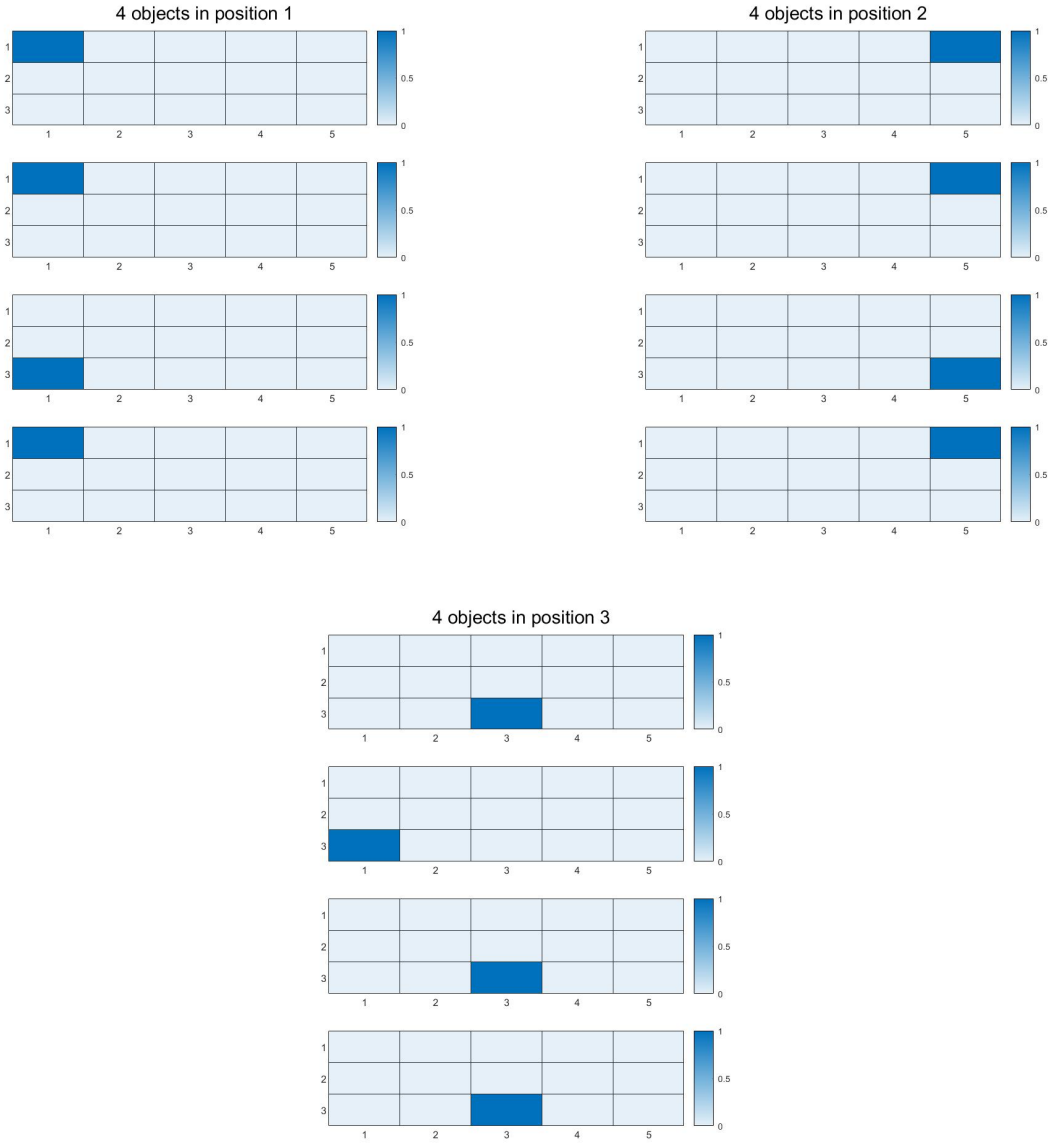


Figure 6-4: Position estimation of four different objects at three positions


Figure 6-5: Attenuation values in each heat map of Figure 6-4

affected. Thus, when the predicted position deviates by one pixel length (in the horizontal direction) or width (in the vertical direction) from the actual position, we still consider the prediction accurate. The results indicate that in the horizontal direction, this system can predict the object's position relatively accurately, yielding consistent results for different test subjects. Only 1 out of 12 estimation is mis-estimated, leading to an accuracy of 91.7%. However, in the vertical direction, although the predicted results consistently fall within the defined range of correct predictions (achieving accuracy rates as high as 91.7% as well), they tend to exhibit relative instability across different test cases. That is, the system could tell whether the object is in the left, right or the middle part of the shelf, but could not achieve a satisfying precision and stability on up, down or middle differentiation. This is mainly because that the overall width of testing region is 32 cm, which raises serious challenges for RF link-based methods, with limitation of radio wavelengths. There are also only three tags on the sides, resulting in less data collected during each measurement. Besides, the objects' sizes are large compared to voxels' size, direct radio link might go through multiple voxels with the same x coordinator but neighboring y coordinator. Thus, when attenuations happen, they could be projected to multiple pixels and increase the likelihood of mis-estimation.

## 6.2 Stocks monitor and auto-stock reminder

With the heatmap generated from position-estimation, some assistive information could be drawn by extracting characteristics.

With the same settings for generating heat map, by comparing the largest attenuation number in the map (where the location estimation is referred to), different stocks could be distinguished. As objects are layered from one to three stacks, the chance of interfering with RF links get increased. However, this also depends on the thickness and size of the objects Figure 6-6, material used in packages and themselves. If the object is too thin, RF links could pass through relative easily and the difference between one and two stacks are not distinct. If the object is too thick, when objects

are stacked into three, the total height is over the height of communication region between antennas and tags, so differences between 2 to 3 stacks could not be detected effectively.


Figure 6-6: Height refence of tested objects, whose length varies from 8cm to 20cm

Below shows heat map when objects with different thickness from 1 to 3 stacks (Figure 6-7, 6-8, 6-9, 6-10, 6-11). Considering objects' thicknesses and sizes, only 1 (milkshake), 2 (animal crackers), 5 (sweetener), 6 (domino's sugar), 7 (pasta box) are measured.

Attenuation for five different objects from 1 to 3 stacks are shown in Figure 6-12. The overall maximum attenuation values have a tendency to increase with number of stacks, which is mostly consistent between all test cases. The relative relationships among attenuation values across different objects serve as indicators of their respective capacities to attenuate RF links. For instance, sugar bags, due to their large size, tend to cause interference with a substantial number of RF links within their proximity. Milk shakes, on the other hand, possess a metal coating within their packaging and contain water, which renders them highly reflective and contributes to their elevated attenuation levels. In contrast, sweeteners and animal crackers exhibit relatively lower attenuation values, primarily attributable to their lack of water content, absence of metal films or other reflective elements, and internal voids. Consequently, these objects behave akin to empty paper shields, resulting in their lower appearance within the provided illustration.

Besides differentiating stacks of object, the overall load on the shelf is also an interesting topic. By summing all attenuation values up, total number of objects on

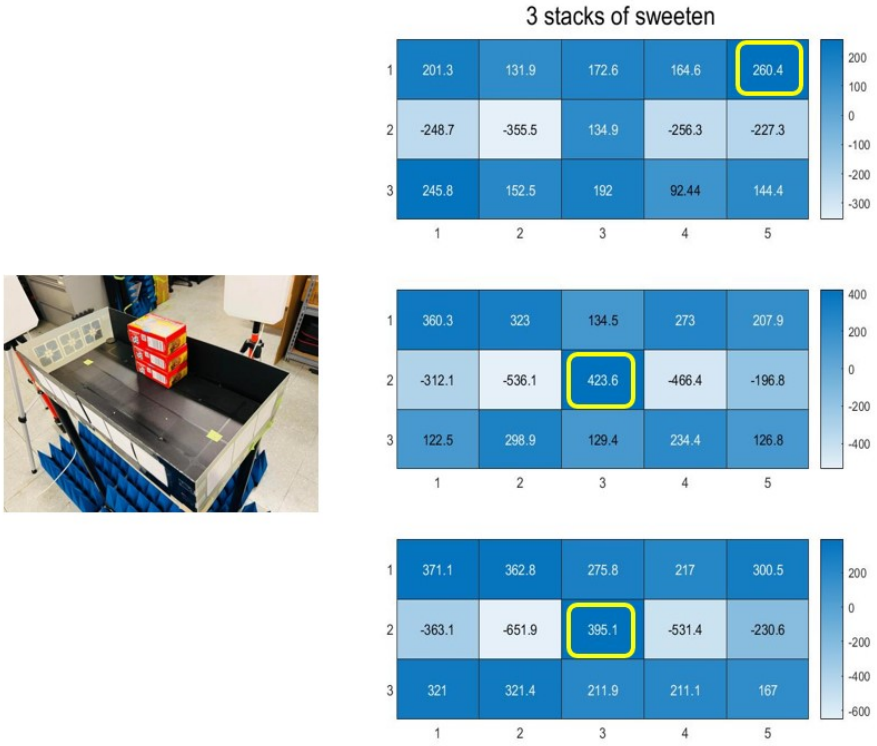


Figure 6-7: Heat map for five different types of objects from 1 to 3 stacks (Animal cracker)

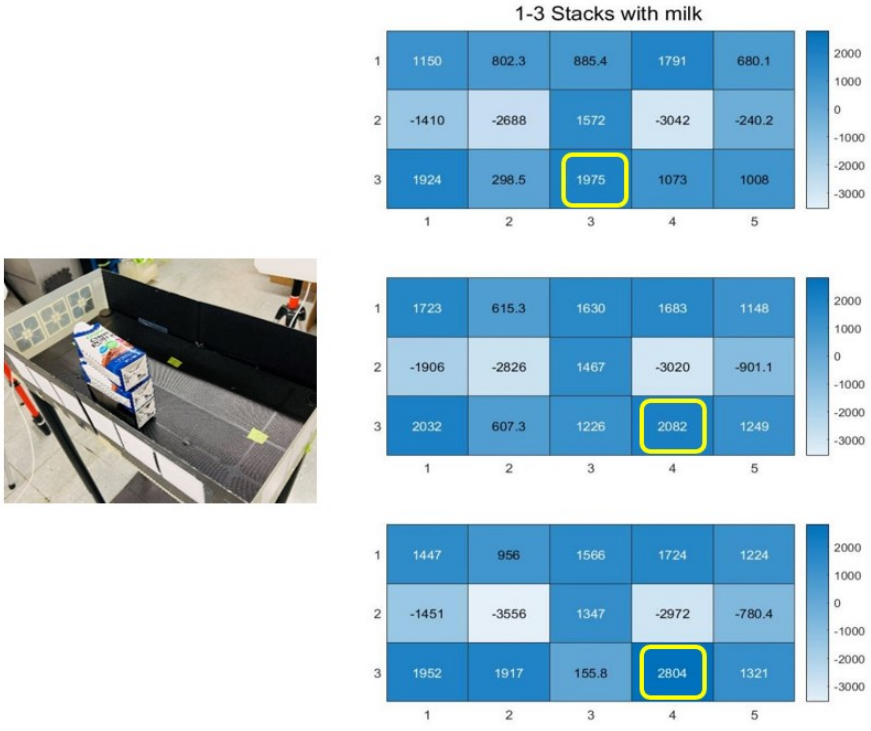


Figure 6-8: Heat map for five different types of objects from 1 to 3 stacks (Milkshake)

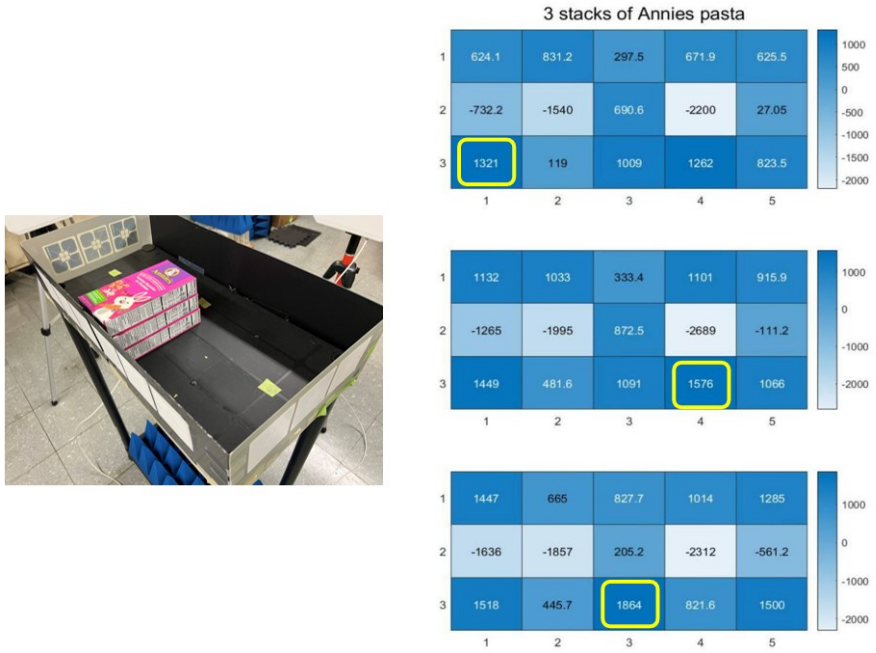


Figure 6-9: Heat map for five different types of objects from 1 to 3 stacks (Pasta)

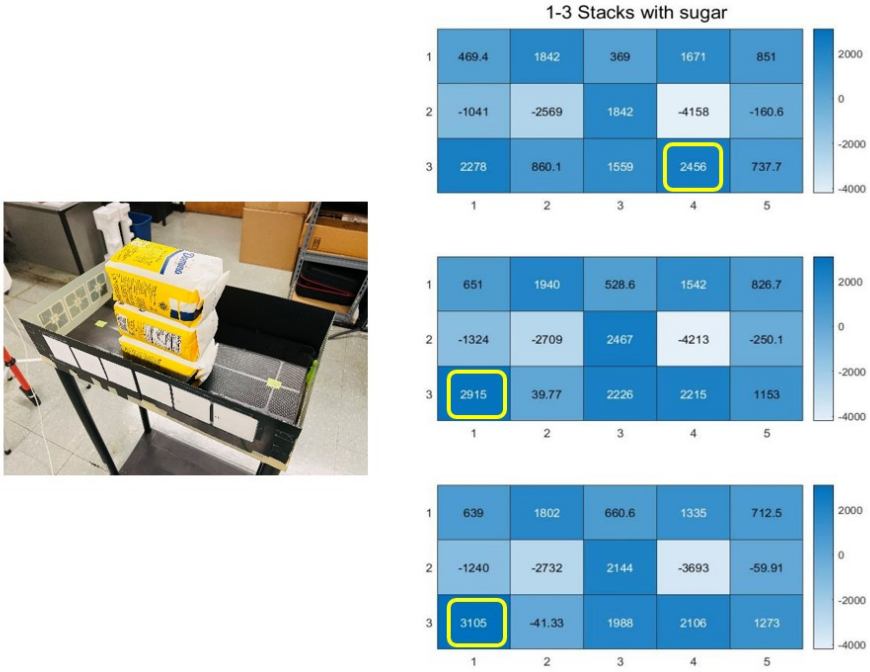


Figure 6-10: Heat map for five different types of objects from 1 to 3 stacks (Sugar)

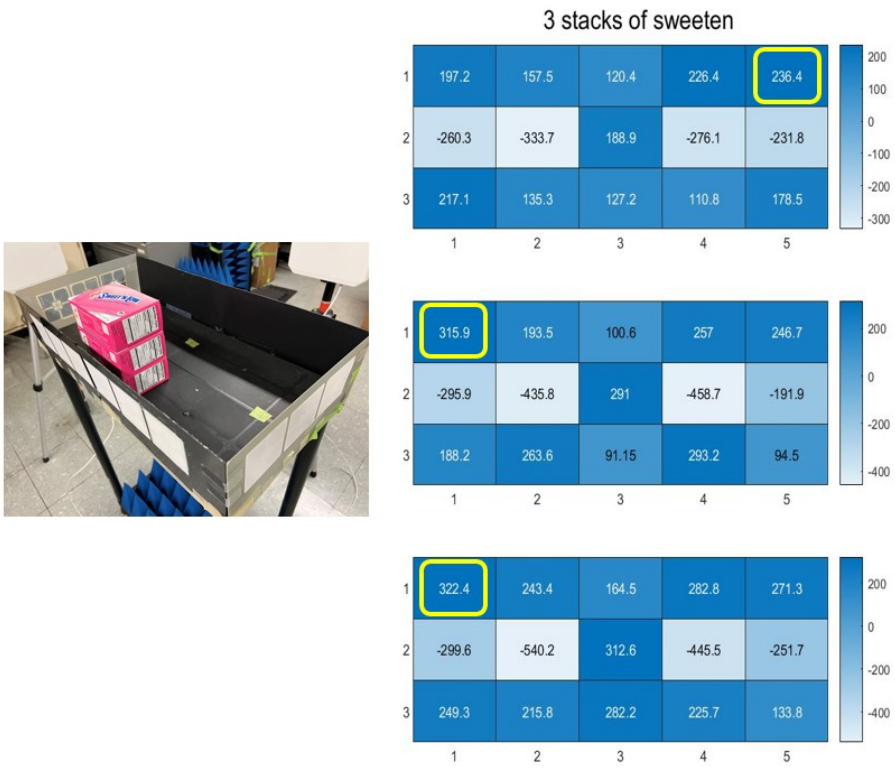


Figure 6-11: Heat map for five different types of objects from 1 to 3 stacks (Sweetener)

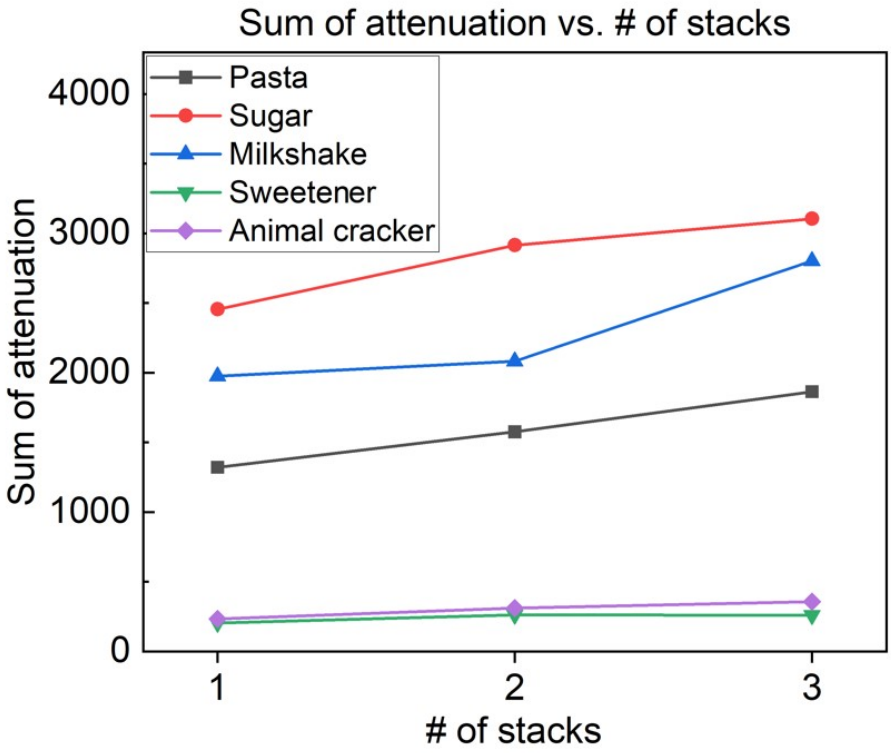


Figure 6-12: Attenuation for five types of objects from 1 to 3 stacks

the shelf could be estimated. Figure 6-13 shows that through the total number of objects increasing from three to nine, the summation also shows an increasing trend. Although it is hard to achieve a monolithic line, this trend could help to generate a qualitative estimation of the overall load on the shelf. Within experiments, three piles are defined and objects are placed from one per pile (3 objects in total) to 3 per pile (9 objects in total) Figure 6-14. Every possible combination to place objects have been measured, and the sum of attenuation is the average value of each combination.

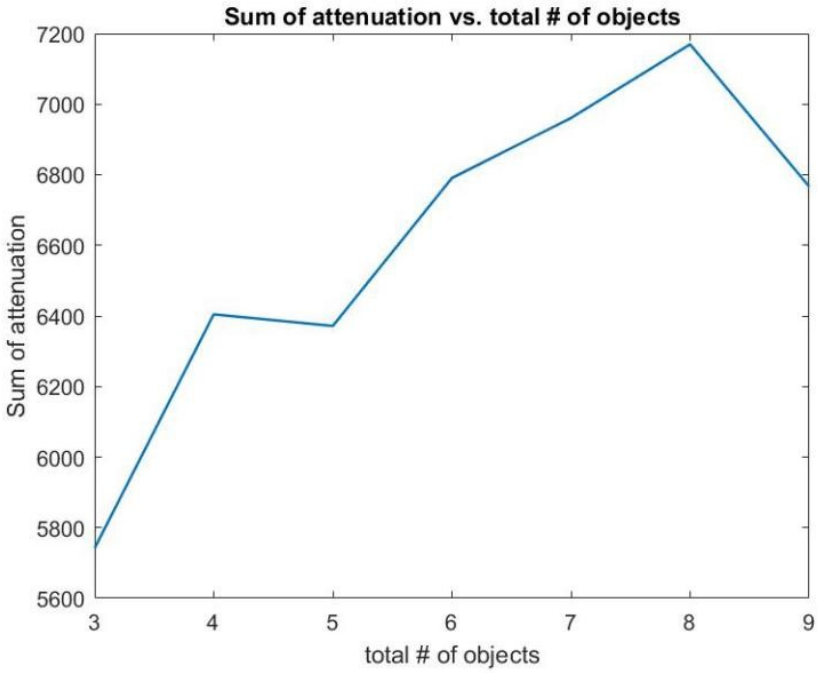


Figure 6-13: Relationship between sum of attenuations and total number of objects on shelf

Figure 6-14: Different numbers of objects being placed on shelf

| % | Position 1 | Position 2 | Position 3 |
|---|---|---|---|
| Plastic | 100 | 100 | 66.7 |
| Glass | 100 | 100 | 100 |
| Metal | 100 | 100 | 100 |

Table 6.1: Location estimations for plastic, glass and metal tested in three locations

## 6.3 Material classification by tag RSSI attenuation

Three types of material (metal, plastic and glass) are measured, each class has three tested objects (Object 1 to 3 from left to right) with similar diameters and sizes Figure 6-15. For each measurement, a specific object with certain material type is placed on one of the three locations, RSSI is recorded for three minutes. Before making material classifications, Figure 6-16, Figure 6-17, Figure 6-18 show the position estimation results for three materials on three positions.


Figure 6-15: Test sets from plastic, glass and metal class

Similar with the first section of the results chapter, estimation results perform more precise and stable in the horizontal direction. By only considering the horizontal estimation, an accuracy matrix of each material is shown in Table 6.1. The overall averaged accuracy is 96.3%. Position estimation of metal objects in position 3 has a shift to the right compared with true position, which probably due to the third position causing more side-effects such as multi-path or fading in the test environment at that time. However, that results remain consistent among three materials and still fall into the range of correct estimation.

Materials are differentiated in dielectric values, which lead to higher or lower attenuations of the same radio path.

Followed by measurements among metal, glass and plastic objects in the previous

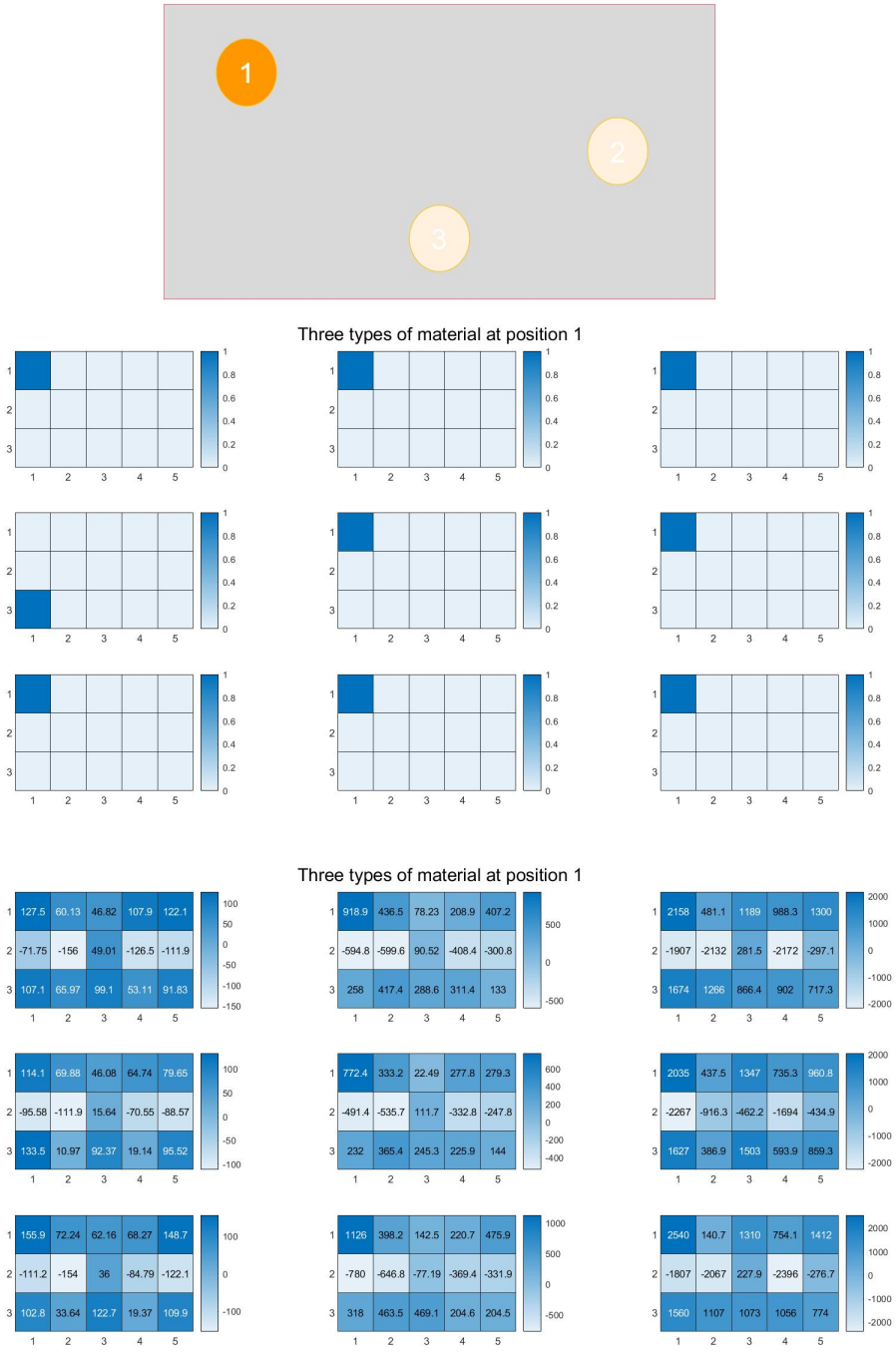


Figure 6-16: Attenuation of three materials (three objects for each material) at position 1

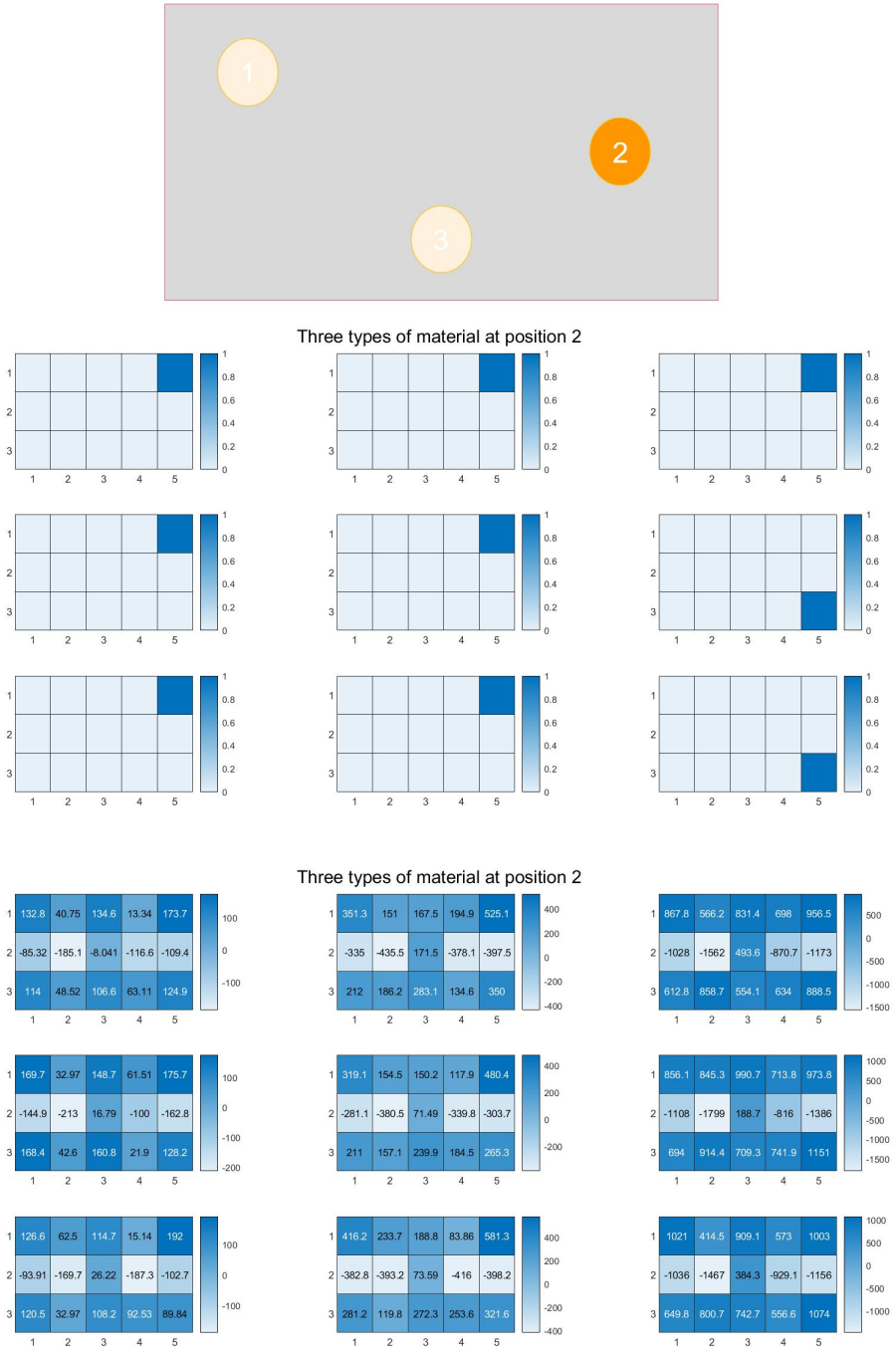


Figure 6-17: Attenuation of three materials (three objects for each material) at position 2

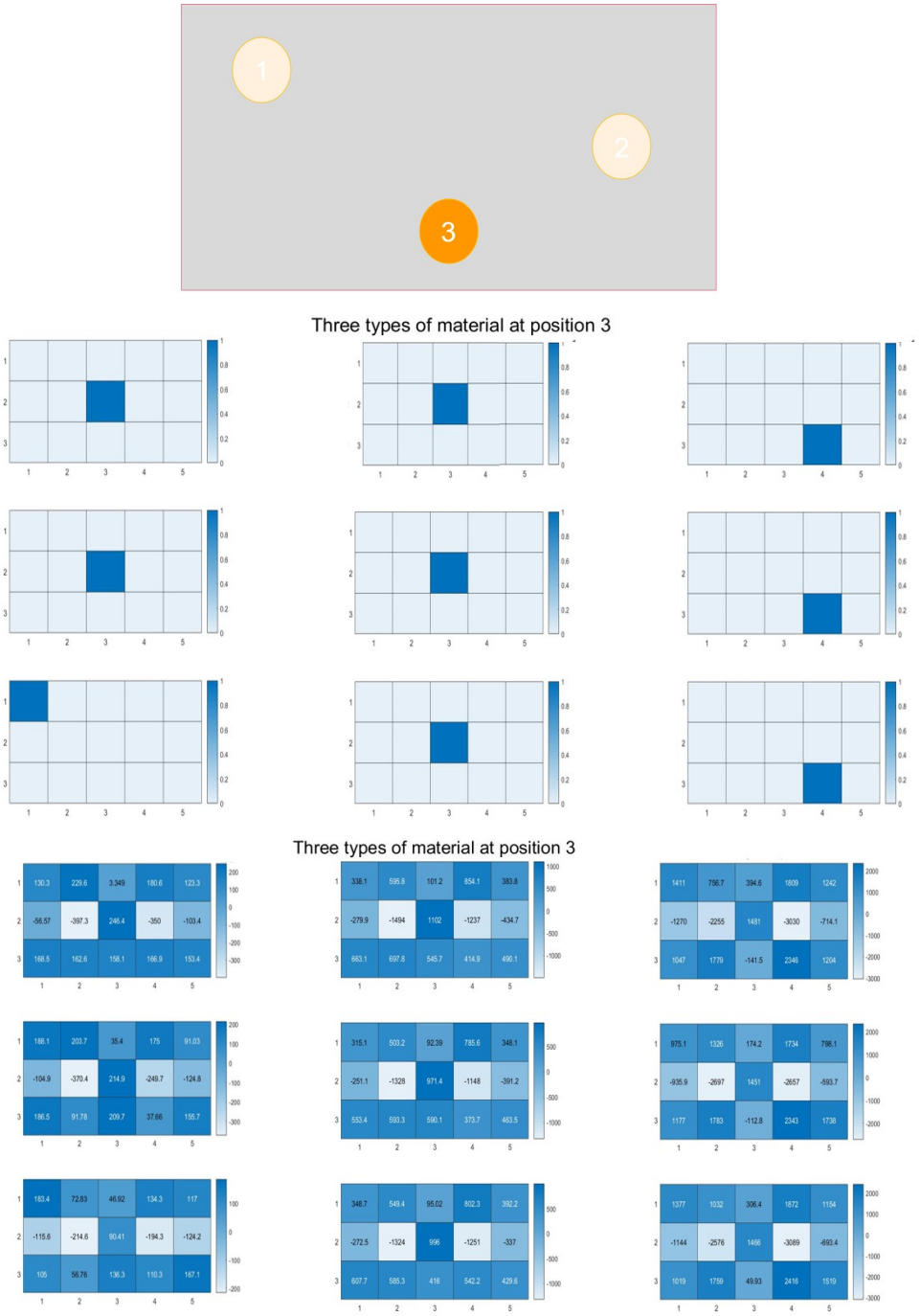


Figure 6-18: Attenuation of three materials (three objects for each material) at position 3

| Averaged max attenuation | Position 1 | Position 2 | Position 3 |
|---|---|---|---|
| Plastic | 139 | 180 | 671.7 |
| Glass | 939.1 | 529 | 1023 |
| Metal | 2244 | 1061 | 2368 |

Table 6.2: Averaged maximum attenuation value for plastic, glass and metal tested in three locations

part, we could make use of attenuation value to get a sense of material composition of the tested object 6-19. Table 6.2 concludes the average attenuation value of the darkest pixel from three-position measurements. When objects are placed in the same position, objects made of the same material result in similar levels of attenuation, while different materials cause significant differences. In the three-location tests, plastic exhibits the lowest attenuation value, while metal generates higher levels of attenuation. This aligns with the dielectric constant and reflective capabilities of metal. Therefore, RF signals can be effectively utilized for material classification.

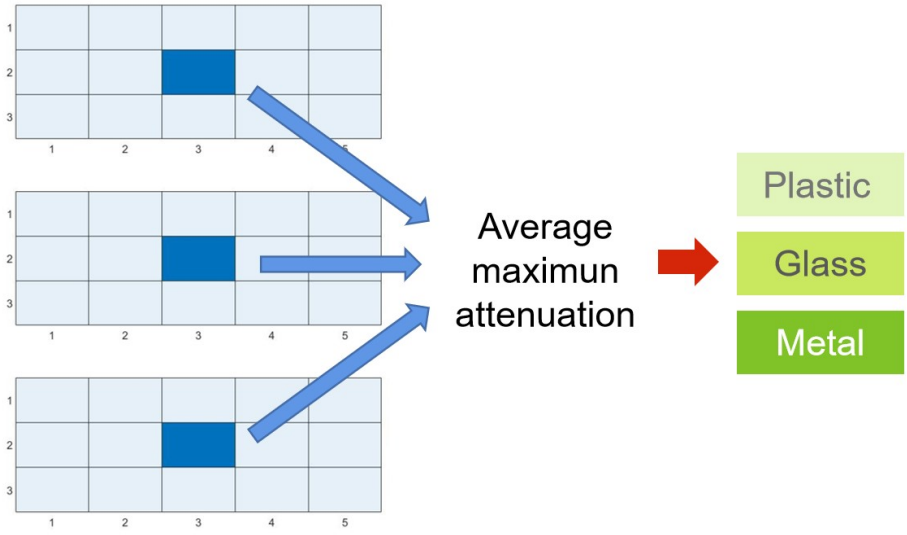


Figure 6-19: By averaging all maximum attenuation values of measurements of one type of material, classifications could be done according to relative relationship between materials.

This is an approach which has small calculation complexity and small commands for memory. However, since it is dependent on relative relationship between materials, it is easily affected by the environment and calibration process is required frequently. In the future, more efforts will be made to eliminate the influence of environmental

factors.

## 6.4 Battery-free environmental sensors

Battery-free RFID sensors, with the advantages of small, lightweight, and cost-effective, can be used to monitor various environmental parameters such as temperature, humidity, pressure, and light. In addition, using RFID technology as environmental sensors is able to operate in real-time. This means that data can be collected and transmitted to a central database immediately, allowing for timely response to environmental changes or anomalies.

Developed by Farsens (which has been bought by Rich RFID in Shenzhen, China), the ROCKY100 chip has gained widespread attention for its unique capabilities and potential applications in various industries. As a passive, battery-less RFID chip, the Rocky 100 offers an efficient and cost-effective solution for wireless data collection and transmission.

The ROCKY100 chip is an EPC Class-1 Generation-2 (C1G2) RFID tag integrated circuit (IC) that adheres to the ISO/IEC 18000-6 Type C standard. This chip offers advanced capabilities, such as sensor measurements and actuator control via SPI communication. It also has a configurable regulated output voltage from LDO regulator and configurable GPIOs to communicate with external devices, triggering operations and retrieving data prior to back-scattering the obtained answer to the reader. The ROCKY100 chip operates a fully passive mode, where it harvests energy from RF bean from the reader. However, it could also work in the Battery Assisted Passive (BAP) mode where an external power source is applied to achieve a better performance.

Serial Peripheral Interface (SPI) communication (Figure 6-20) is a widely used synchronous communication protocol that enables data exchange between microcontrollers, sensors, and other peripheral devices in embedded systems. In SPI communication, data is transmitted in a master-slave configuration, where one device acts as the master, controlling the communication, and one or more devices function as

slaves, responding to the master's commands. The master device initiates communication by generating a clock signal and transmitting data bits in a serial format, while the slave devices receive and respond to the data.

As a SPI master device, ROCKY100 could communicate with slave device with four wires:

- CS: Chip Select signal to enable the slave device, driven by the SPI master.
- SCK: Serial Clock, driven by the SPI master.
- MOSI: Master Output Slave Input data port, driven by the SPI master.
- MISO: Master Input Slave Output data port, driven by the SPI slave.

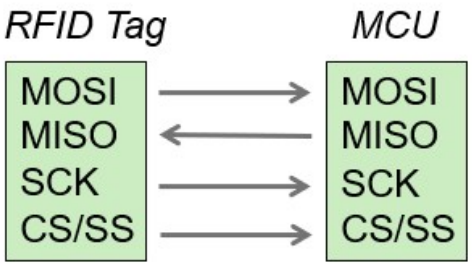


Figure 6-20: SPI protocol

To initiate the communication, read command in RFID protocol is needed by specifying Memory Bank, Word Pointer and Word Count.

In ROCKY100's memory, the SPI bridge is corresponded to any memory address starting from CURRENT_SBA (SPI Base Address) in the User memory bank. By default, CURRENT_SBA is 0x06 and the data stored in 0x06 is 0x100 (This could be altered by Write into address 0x06 the new data through C1G2. That is to say, by reading from the address 0x100 of the User bank, ROCKY100 could start a SPI communication as Master and could get response from Slave as the content of some specific memory addresses.

On the hardware side, to build up a sensing platform, ROCKY100 is usually connected with a micro-controller (MCU) via SPI wires (mentioned above), which

is controlling one or multiple sensors Figure 6-21. Farsens developed several RFID wireless battery free sensors with ROCKY100. For example, the RMETER-RM tag, which is a battery-less resistance sensor, consists of a ROCKY100 IC for energy harvesting and wireless communication, a micro-controller with integrated ADC (12 bits) and signal conditioning circuitry for measuring resistive sensors.


Figure 6-21: Communication within RFID sensor

Two approaches are applied to read from a RFID tag's memory. The first one is through the Impinj's demo software ItemTest [49] (Figure 6-22) that can be used with all Impinj RFID readers. In ItemTest, after entering the memory of this chip (by acknowledging its specific EPC), user could read certain words in certain memory bank and address (Figure 6-23).

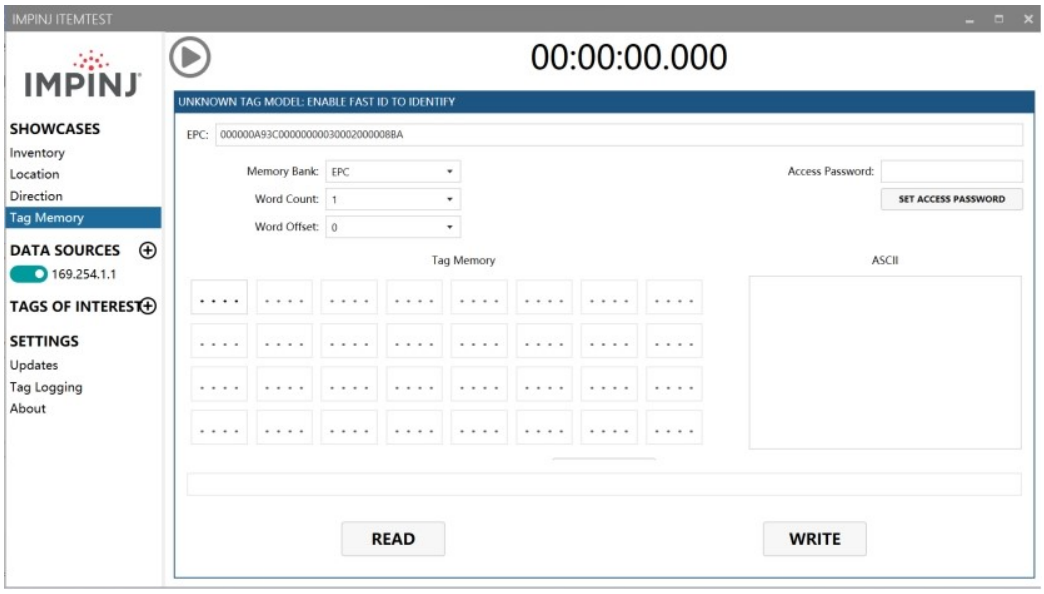


Figure 6-22: In Impinj software, user could read contents from a tag's memory after specifying EPC of the tag.

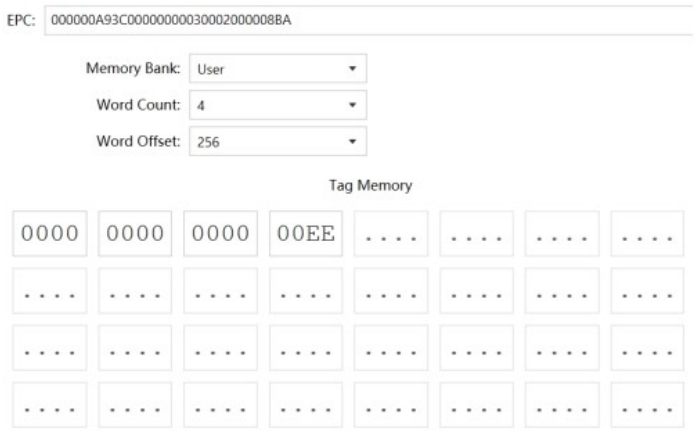


Figure 6-23: Example of reading 4 words start from address 256 from User bank

The second approach to read from tag's memory is using Octane SDK which is a development library that support *C#* and Java applications for Impinj RAIN RFID readers and gateways.

By specifying the memory bank, word count and word offset to "User", "4" and "256" (decimal of 0x100), data acquired by sensors could be obtained (Figure 6-24). Note that reading results are encoded in single precision floating point format (Little Endian). According to tag's design, two QOS bits which indicated the validity of sensor data will be embedded in reading results (Figure 6-25).

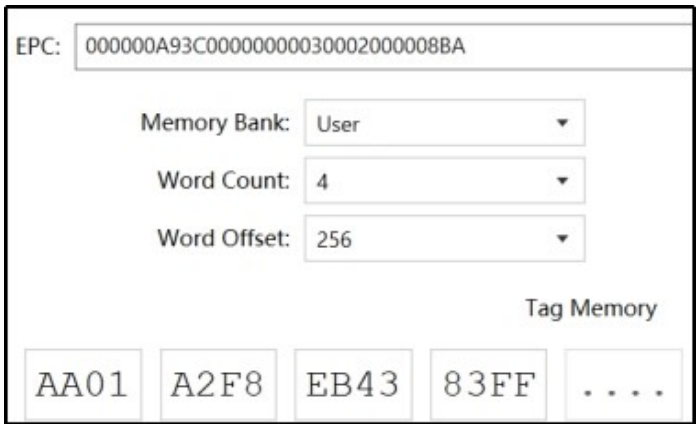


Figure 6-24: Example of a valid resistance measurement data with ItemTest

With the resistance sensor, a new approach is raised to monitor the overall load situation on shelf together with a photoresistor, by monitoring the light intensity which would alter with the total number of objects on the shelf.

| QOS | Meaning |
|---|---|
| 0xFF | Sensor working in best conditions |
| 0xEE | Sensor working in good conditions |
| 0xCC | Sensor switched off |
| 0x88 | Sensor switched off |

Figure 6-25: QOS bits could indicate the validity of sensor data.

A photoresistor is a passive electronic component that exhibits a reduction in resistance proportional to the intensity of incident light on its sensitive surface. The behavior of a photoresistor is characterized by a decrease in resistance as the incident light intensity increases. When the incident light surpasses a specific frequency threshold, photons absorbed by the semiconductor material provide sufficient energy for bound electrons to transition into the conduction band. As a result, free electrons, along with their corresponding holes, facilitate the conduction of electricity, leading to a decrease in resistance. It is important to note that the resistance range and sensitivity of a photoresistor can vary significantly across different devices. Additionally, unique photoresistors may exhibit diverse responses to photons within specific wavelength ranges.

In the proposed sensing system, the Rocky100 based resistance sensor is connected to a photoresistor with 2-5 kohm Figure 6-26 and these elements are put in the backside of the shelf. The shelf is placed against the wall, which controls lighting on the shelf surface to only come from the front and both sides Figure 6-27. Firstly, the system is tested in different environment lighting, such as with light on/off, w/o flashlight of cellphone shining directly from near or far distance. Since the resistance sensor is compatible with commercial UHF RFID readers (through C1G2), lighting situation could be detected by reading operations with Impinj R420 reader. Results shows that it could manage to differentiate among environment lighting Figure 6-28.

Regarding to the shelf region, while putting more and more stuffs on the shelf Figure 6-29, more shadows are predicted to be generated and decrease the overall light on the photoresistor. This leads to its resistance changing. Figure 6-30 shows the resistance when one to three stacks of boxes are placed in front of light sensor.

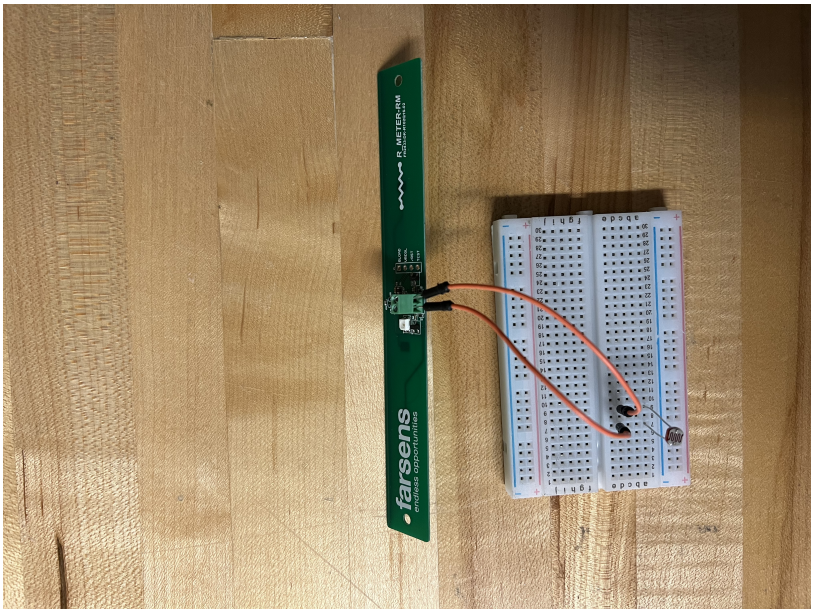


Figure 6-26: Rocky100 connected to a photoresistor

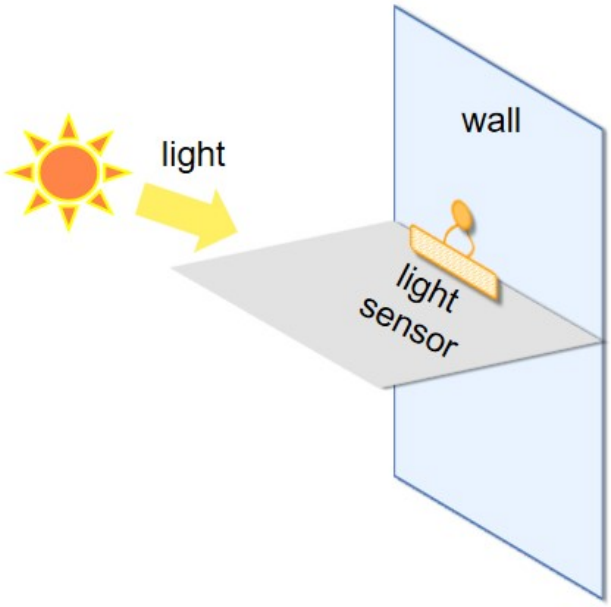


Figure 6-27: Placement of light sensor and direction of light

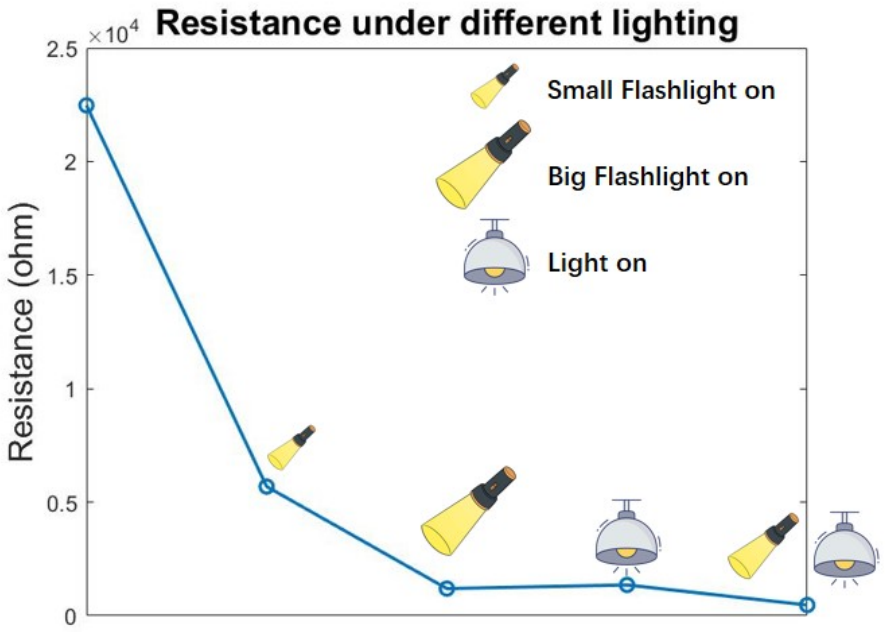


Figure 6-28: Resistance of photoresistor under different lighting. Small flashlight means taking the flashlight of cellphone away at around 50 cm and shine at the photoresistor. Big flashlight means that it shines from close up at the sensor.

There is an obvious jump between one and two stacks, which is mainly caused by direct shadow on photoresistor after one layer is added to two layers. It is worthy to note that despite one layer doesn't generate shadow on photoresistor, it will still absorb, reflect or scatter some light from the light source, which will also increase resistance of photoresistor. This shows that this light sensor is sensitive enough to detect lighting changes which are not detectable by observing shadow positions.

For further explore the light sensor, Figure 6-31 shows the change of photoresistor resistance when various number of objects are put on the shelf. There are three piles of objects on the shelf, with a total number of objects ranging from 3 to 9. For each specific total number of objects, three combinations were measured, and the final resistance value was obtained by taking the measured values of resistance for these three combinations. When determining the combinations, for a total of 4-6 objects, the highest pile does not exceed two objects; for a total of 7-9 objects, the highest pile has three objects. This is because in real-life shelf arrangements, each type of goods has a fixed display area, and we assume that the salesperson prefers to place

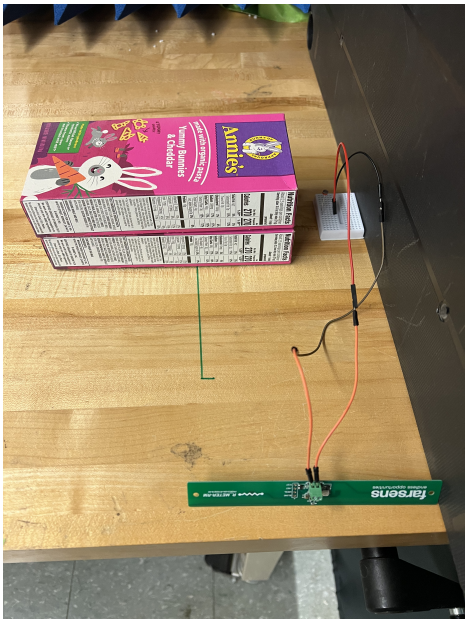


Figure 6-29: Situation when two stacks of boxes are placed in front of the photoresistor

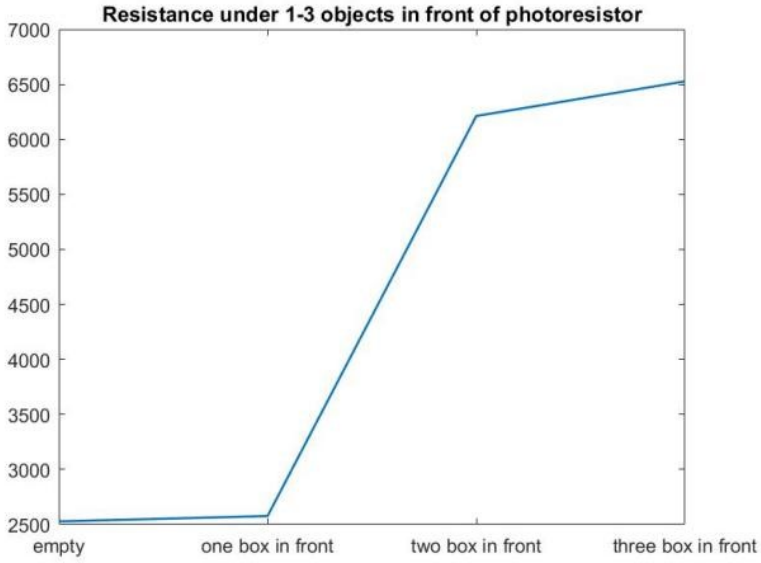


Figure 6-30: Resistance of photoresistor when one to three stacks of boxes are placed in the front

the goods evenly rather than have one pile be significantly taller or shorter than the others. For example, for total number of 5, combinations could be (1,2,2), (2,1,2) and (2,2,1) from left to right. Figure 6-32 shows examples of different compositions with total number of 6 objects.

From Figure 6-31, it can be observed that although the number of objects in the middle pile (which has the greatest impact on the resistance value) varies, the overall resistance value still increases as the total number of objects increases. This is because that the total number has a relationship with stack number of the middle pile. Additionally, the influence of the adjacent piles on the light transmission also plays a role. Based on the data from the average of the three combinations, the final resistance value can provide an qualitative estimation of the overall inventory and the highest layer of objects on the shelf. In future work, with multiple light sensors in the back, more quantitative data can be obtained.

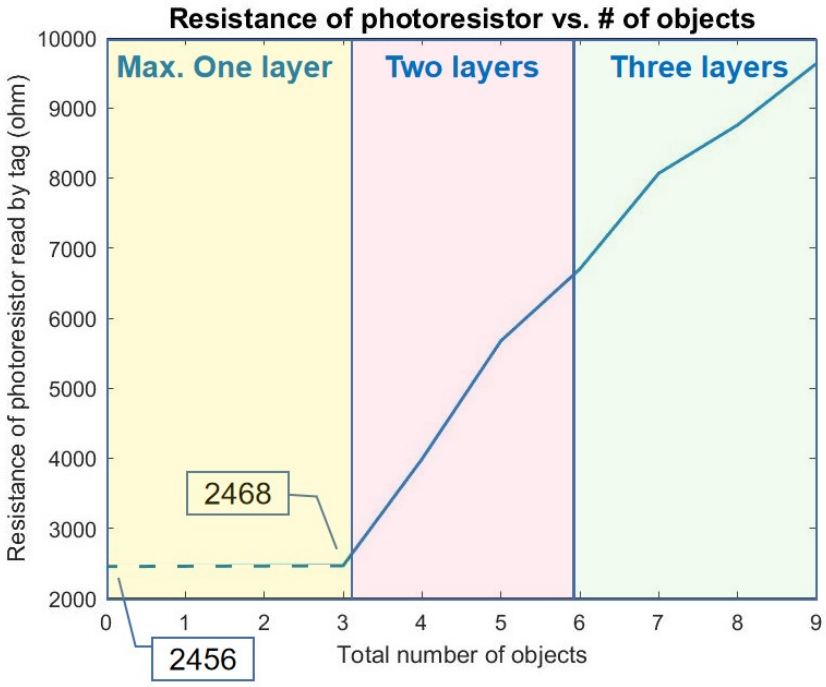


Figure 6-31: Resistance vs. total number of objects. Numbers could also indicate the maximum layer on the shelf.

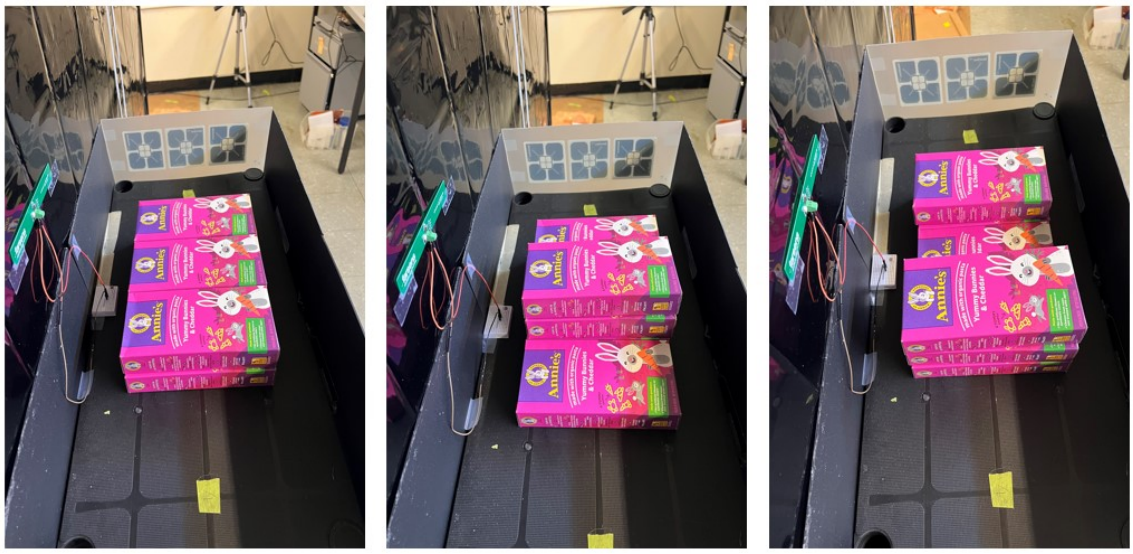


Figure 6-32: Three tested combinations for total number of 6 objects

# Chapter 7

# Conclusions and future work

## 7.1 Conclusion

In this thesis, a smart shelf with context awareness is built using passive UHF RFID and the RTI algorithm. First, a non-fingerprinting method was employed to estimate the positions of objects on the shelf. Experiments were conducted with four different objects at three locations. Estimation accuracy in both horizontal and vertical direction reach 96.3% while horizontal estimation is with larger stability and precision.

Furthermore, by summing all the attenuation numbers on the heat map, the number of layers at which an object is placed on the shelf can be determined. Five different products were tested, and as the number of layers increased from one to three, this value showed a monotonically increasing trend.

Testings were also performed on three materials (metal, glass, plastic) from the same three positions. The mean location estimation accuracy for all test cases is 96.3%. After generating a heat map, the type of material can also be detected by examining the maximum attenuation value. Objects from the same material class exhibit similar attenuation values, while there is a significant difference between different materials. This characteristic can be utilized for material classification.

Lastly, battery-free environmental sensors are designed to be integrated by adding an RFID tag capable of resistance measurement and a photoresistor. Assuming there are three piles of objects on the shelf, the total number of objects on the shelf and

the highest number of layers can be estimated by measuring the resistance of the photoresistor.

## 7.2 Future work

In order to further substantiate the conclusions presented in this study regarding the various trends discussed, including position detection, material identification, and stack analysis, it is advisable to conduct additional experiments. For instance, modifying the testing environment to vary its level of reflectivity would provide valuable insights. The work of material classification using tag RSSI attenuation can also be further generalized to eliminate the influence of environmental factors.

Furthermore, the analysis of heat maps through filtering or differentiation of the original heat map may offer the potential to determine the metallic composition of products on a shelf. By discerning the patterns of pixel changes, it is hypothesized that the presence of metal, which can interfere with RF fields, could lead to less stable heat maps across pixels. This technique shows promise in detecting instances where consumers have misplaced certain product types. Nonetheless, further research is required to validate and refine these findings.

The current outcomes are predicated on the assumption that all nodes are situated within the same plane, thereby resulting in two-dimensional information. However, practical scenarios involve a third dimension, and computer vision algorithms often encounter difficulties in acquiring depth information. To surmount this limitation, the installation of additional antennas in a perpendicular direction would establish RF links in an alternative plane. Expanding the system in this manner would enable the retrieval of supplementary information, such as object height and shape.

On the sensing aspect, similar approaches can be applied to simultaneously control multiple sensors utilizing a unified protocol and RF communication. This would facilitate the detection of environmental parameters, including temperature, humidity, and pressure, based on specific requirements. Additionally, employing the SPI protocol enables the control of actuators, significantly broadening the range of potential

applications. One notable example is the utilization of digital labels, which offer enhanced dynamism and flexibility in presenting product information and pricing within retail stores. Kroger has successfully employed digital shelf-edge technology to display product prices, promotions, and nutritional information. By sending commands from an RFID reader, multiple tasks can be orchestrated and executed efficiently.

Finally, power harvesting remains a significant concern in the context of passive RFID applications. The exploration of various techniques for power harvesting, particularly in relation to sensors, represents a significant area for further investigation and advancement.

# Bibliography


[1] Peter C. Verhoef, P.K. Kannan, and J. Jeffrey Inman. From multi-channel retailing to omni-channel retailing: Introduction to the special issue on multi-channel retailing. *Journal of Retailing*, 91(2):174–181, 2015. Multi-Channel Retailing.

[2] Glenn R. Cook. Customer experience in the omni-channel world and the challenges and opportunities this presents. *Journal of Direct, Data and Digital Marketing Practice*, 15:262–266, 2014.

[3] Marco Melacini, Sara Perotti, Monica Rasini, and Elena Tappia. E-fulfilment and distribution in omni-channel retailing: a systematic literature review. *International Journal of Physical Distribution  Logistics Management*, 48, 04 2018.

[4] Syed Raza and Srikrishna Govindaluri. Omni-channel retailing in supply chains: a systematic literature review. *Benchmarking An International Journal*, ahead-of-print, 02 2021.

[5] Holly Briedis, Brian Gregg, Kevin Heidenreich, and Wei Wei Liu. Omnichannel: The path to value, Apr 2021.

[6] Simone Aiolfi and Edoardo Sabbadin. The new paradigm of the omnichannel retailing: Key drivers, new challenges and potential outcomes resulting from the adoption of an omnichannel approach. *International Journal of Business and Management*, 13:85, 12 2017.

[7] Chris Lazaris, Adam Vrechopoulos, Katerina Fraidaki, and Georgios Doukidis. Exploring the "omnichannel" shopper behaviour. In *AMA SERVSIG, International Service Research Conference*, pages 13–15, 2014.

[8] Carla R. Medeiros, Jorge R. Costa, and Carlos A. Fernandes. Rfid smart shelf with confined detection volume at uhf. *IEEE Antennas and Wireless Propagation Letters*, 7:773–776, 2008.

[9] Florin Hrebenciuc, Stroia Nicoleta, Daniel Moga, and Zsolt Barabas. A low cost approach to large smart shelf setups. *Advances in Electrical and Computer Engineering*, 11:117–122, 11 2011.

[10] Joan Melià-Seguí and Rafael Pous. Human-object interaction reasoning using rfid-enabled smart shelf. In *2014 International Conference on the Internet of Things (IOT)*, pages 37–42, 2014.

[11] Bikash Santra and Dipti Prasad Mukherjee. A comprehensive survey on computer vision based approaches for automatic identification of products in retail store. *Image and Vision Computing*, 86:45–63, 2019.

[12] Xiaohua Shi, Kaicheng Tang, and Hongtao Lu. Smart library book sorting application with intelligence computer vision technology. *Library Hi Tech*, ahead-of-print, 04 2020.

[13] Christian Koch, Kristina Georgieva, Varun Kasireddy, Burcu Akinci, and Paul Fieguth. A review on computer vision based defect detection and condition assessment of concrete and asphalt civil infrastructure. *Advanced Engineering Informatics*, 29(2):196–210, 2015.

[14] Achuta Kadambi, Ayush Bhandari, and Ramesh Raskar. 3d depth cameras in vision: Benefits and limitations of the hardware: With an emphasis on the first- and second-generation kinect models. *Computer vision and machine learning with RGB-D sensors*, pages 3–26, 2014.

[15] Hanchuan Li, Peijin Zhang, Samer Al Moubayed, Shwetak N. Patel, and Alanson P. Sample. Id-match: A hybrid computer vision and rfid system for recognizing individuals in groups. In *Proceedings of the 2016 CHI Conference on Human Factors in Computing Systems*, CHI '16, pages 4933–4944, New York, NY, USA, 2016. ACM.

[16] Rong-Shue Hsiao, C.-H Kao, Hsin-Piao Lin, and Kai-Wei Ke. Improving radio frequency identification-based localization accuracy using computer-vision-assisted sensor deployment technology. *Sensors and Materials*, 29:387–395, 01 2017.

[17] Chunhui Duan, Xing Rao, Lei Yang, and Yunhao Liu. Fusing rfid and computer vision for fine-grained object tracking. In *IEEE INFOCOM 2017 - IEEE Conference on Computer Communications*, pages 1–9, 2017.

[18] Felix Weber and Reinhard Schütte. State-of-the-art and adoption of artificial intelligence in retailing. *Digital Policy, Regulation and Governance*, 21, 05 2019.

[19] Ashish Ghosh, Debasrita Chakraborty, and Anwesha Law. Artificial intelligence in internet of things. *CAAI Transactions on Intelligence Technology*, 3, 10 2018.

[20] Nadya Istiqomah, Putri Sansabilla, Doddy Himawan, and Muhammad Rifni. The implementation of barcode on warehouse management system for warehouse efficiency. *Journal of Physics: Conference Series*, 1573:012038, 07 2020.

[21] R. L. Ballard. Methods of inventory monitoring and measurement. *Logistics Information Management*, 9:11–18, 1996.

[22] Patricia J. Daugherty, Matthew B. Myers, and Chad W. Autry. Automatic replenishment programs: An empirical examination. *Journal of Business Logistics*, 20(2):63–82, 1999.

[23] Sathish Paulraj Gundupalli, Subrata Hait, and Atul Thakur. A review on automated sorting of source-separated municipal solid waste for recycling. *Waste Management*, 60:56–74, 2017. Special Thematic Issue: Urban Mining and Circular Economy.

[24] Yu Zheng, Siqi Qiu, Fei Shen, and Changpeng He. Rfid-based material delivery method for mixed-model automobile assembly. *Computers Industrial Engineering*, 139:106023, 2020.

[25] Aobo Zhao, Ali Imam Sunny, Li Li, and Tengjiao Wang. Machine learning-based structural health monitoring using rfid for harsh environmental conditions. *Electronics*, 11(11), 2022.

[26] Haoyan Huo, Ziqin Rong, Olga Kononova, Wenhao Sun, Tiago Botari, Tanjin He, Vahe Tshitoyan, and Gerbrand Ceder. Semi-supervised machine-learning classification of materials synthesis procedures. *npj Computational Materials*, 5:62, 07 2019.

[27] Chenyang Li, Lingfei Mo, and Dongkai Zhang. Review on uhf rfid localization methods. *IEEE Journal of Radio Frequency Identification*, 3(4):205–215, 2019.

[28] Jeffrey Hightower, Roy Want, and Gaetano Borriello. Spoton: An indoor 3d location sensing technology based on rf signal strength. 2000.

[29] Jing Yuan, Xuegang Wang, Liang Dong, Ning Li, Fu Wang, Yalou Huang, Fengchi Sun, and Yuan Wang. Isilon-an intelligent system for indoor localization and navigation based on rfid and ultrasonic techniques. 07 2010.

[30] Tianzhu Qiao, Yu Zhang, and Huaping Liu. Nonlinear expectation maximization estimator for tdoa localization. *IEEE Wireless Communications Letters*, 3(6):637–640, 2014.

[31] Yi Zhao and Joshua R. Smith. A battery-free rfid-based indoor acoustic localization platform. In *2013 IEEE International Conference on RFID (RFID)*, pages 110–117, 2013.

[32] Ales Povalac and Jiri Sebesta. Phase difference of arrival distance estimation for rfid tags in frequency domain. In *2011 IEEE International Conference on RFID-Technologies and Applications*, pages 188–193, 2011.

[33] Joey Wilson and Neal Patwari. Radio tomographic imaging with wireless networks. *IEEE Trans. Mob. Comput.*, 9:621–632, 01 2010.

[34] Xin Xiao, Xiaojun Jing, Siqing You, and Jian Zeng. An environmental-adaptive rssi based indoor positioning approach using rfid. In *2010 International Conference on Advanced Intelligence and Awarenss Internet (AIAI 2010)*, pages 127–130, 2010.

[35] Daqiang Zhang, Jingyu Zhou, Minyi Guo, Jiannong Cao, and Tianbao Li. Tasa: Tag-free activity sensing using rfid tag arrays. *IEEE Transactions on Parallel and Distributed Systems*, 22(4):558–570, 2011.

[36] Elham Moradi, Karoliina Koski, Leena Ukkonen, Yahya Rahmat-Samii, Toni Björninen, and Lauri Sydänheimo. Embroidered rfid tags in body-centric communication. In *2013 International Workshop on Antenna Technology (iWAT)*, pages 367–370. IEEE, 2013.

[37] Newton SSM Da Fonseca, Raimundo CS Freire, Adriano Batista, Glauco Fontgalland, and Smail Tedjini. A passive capacitive soil moisture and environment temperature uhf rfid based sensor for low cost agricultural applications. In *2017 SBMO/IEEE MTT-S International Microwave and Optoelectronics Conference (IMOC)*, pages 1–4. IEEE, 2017.

[38] AMSSLAEP Class. Sensory tag chip—for automatic data logging datasheet, ams. october 2018, 3.

[39] José Fernández Salmerón, Francisco Molina-Lopez, Almudena Rivadeneyra, Andrés Vásquez Quintero, Luis Fermin Capitán-Vallvey, Nico F de Rooij, Jesús Banqueri Ozáez, Danick Briand, and Alberto J Palma. Design and development of sensing rfid tags on flexible foil compatible with epc gen 2. *IEEE Sensors Journal*, 14(12):4361–4371, 2014.

[40] L. Catarinucci, D. De Donno, L. Mainetti, L. Palano, L. Patrono, M. L. Stefanizzi, and L. Tarricone. Integration of uhf rfid and wsn technologies in healthcare systems. In *2014 IEEE RFID Technology and Applications Conference (RFID-TA)*, pages 289–294, 2014.

[41] Daniel Dobkin. *The rf in RFID: uhf RFID in practice*. Newnes, 2012.

[42] Chenglong Li, Emmeric Tanghe, David Plets, Pieter Suanet, Jeroen Hoebeke, Eli De Poorter, and Wout Joseph. Reloc: Hybrid rssi- and phase-based relative uhf-rfid tag localization with cots devices. *IEEE Transactions on Instrumentation and Measurement*, 69(10):8613–8627, 2020.

[43] Zheng Liu, Zhe Fu, Tongyun Li, Ian White, Richard Penty, and Michael Crisp. A fast phase and rssi-based localization method using passive rid system with mobile platform. In *2021 IEEE International Conference on RFID Technology and Applications (RFID-TA)*, pages 48–51, 2021.

[44] Benjamin Wagner, Nihal Patwari, and Dirk Timmermann. Passive rfid tomographic imaging for device-free user localization. pages 120–125, 03 2012.

[45] Neal Patwari and Piyush Agrawal. Effects of correlated shadowing: Connectivity, localization, and rf tomography. In *2008 International Conference on Information Processing in Sensor Networks (ipsn 2008)*, pages 82–93, 2008.

[46] Joey Wilson, Neal Patwari, and Fernando Guevara Vasquez. Regularization methods for radio tomographic imaging. In *2009 Virginia Tech Symposium on Wireless Personal Communications*. Citeseer Princeton, NJ, USA, 2009.

[47] Corey Cooke. *Attenuation field estimation using radio tomography*. PhD thesis, Virginia Tech, 2011.

[48] Neal Patwari, Lara Brewer, Quinn Tate, Ossi Kaltiokallio, and Maurizio Bocca. Breathfinding: A wireless network that monitors and locates breathing in a home. *IEEE Journal of Selected Topics in Signal Processing*, 8(1):30–42, 2014.

[49] Impinj itemtest software. https://support.impinj.com/hc/en-us/articles/204059593-Impinj-ItemTest-Software.